Trends in Analytical Chemistry 158 (2023) 116858

Contents lists available at ScienceDirect

Trends in Analytical Chemistry

journal homepage: www.elsevier.com/locate/trac

Microfluidic bioanalysis based on nanozymes

Quanyi Liu [a, b], Hui Wei [c, d, **], Yan Du [a, b, *]

[a] State Key Laboratory of Electroanalytical Chemistry, Changchun Institute of Applied Chemistry, Chinese Academy of Sciences, Changchun, Jilin, 130022, China
[b] University of Science and Technology of China, Hefei, Anhui, 230026, China
[c] College of Engineering and Applied Sciences, Nanjing National Laboratory of Microstructures, Jiangsu Key Laboratory of Artificial Functional Materials, Nanjing University, Nanjing, Jiangsu, 210023, China
[d] State Key Laboratory of Analytical Chemistry for Life Science, School of Chemistry and Chemical Engineering, Chemistry and Biomedicine Innovation Center (ChemBIC), Nanjing University, Nanjing, Jiangsu, 210023, China

ARTICLE INFO

Article history:
Received 27 August 2022
Received in revised form
21 November 2022
Accepted 23 November 2022
Available online 7 December 2022

Keywords:
Nanozyme
Bioanalysis
Microfluidics
Paper-based microfluidic
Point-of-care testing

ABSTRACT

As a powerful tool, microfluidics has been widely used in bioanalysis due to the advantages of high portability, fewer sample requirements and rapid detection time. To achieve selective and sensitive detection, enzymes are commonly used as biorecognition elements. However, enzymes used in bioanalysis still suffer from high cost and low stability. Therefore, emerging nanozymes (nanomaterials with enzyme-like characteristics) have been developed to replace enzymes to address their shortcomings. The microfluidic devices based on nanozymes have attracted a lot of interest and shown great promise in bioanalysis via a simple, rapid, and portable approach. This review focuses on recent advances in typical nanozymes and nanozymes involved in cascaded reactions used in microfluidic bioanalysis. Additionally, the future challenges and perspectives are discussed for further development.

1. Introduction

The monitoring of human health has always been the goal of precise analysis of biological molecules [1]. The pursuit of reliable methods for quantitating drugs and their metabolites is also an important part for disease treatment. Therefore, a series of classical bioanalysis technologies have been developed, such as high-performance liquid chromatography (HPLC) and liquid chromatography tandem mass spectrometry (LC-MS/MS) [2,3]. However, many conventional bioanalysis methods have been limited by large sample volumes, long waiting times and high cost of professional equipment. As an emerging technology, microfluidics has been regarded as a crucial technology in various fields, ranging from material science to biomedical engineering [4–6]. In typical microfluidics, minute amounts of fluids are manipulated at the micron scale to perform precise sample preparation, reaction, separation, and evaluation [7]. Benefiting from their excellent performance, it is much more accessible to synthesize particles with controlled morphologies and compositions [8]. Moreover, the microfluidic system, also known as miniaturized total analysis system (μTAS) or lab-on-a-chip (LOC), has also been considered as a powerful analytical tool due to its advantages of portability, reduced amount of sample, rapid reaction time and less need for large equipment [6]. Based on this microfluidic technology, lots of unprecedented bioanalyses have been advanced with low cost, high accuracy, high resolution, and simple operation [4,9,10]. And the microfluidic devices have been applied in many important areas, such as biomarker detection, high-throughput drug screening, single cell analysis, and genomic sequencing [4].

Though various novel analytical methods have been expanded in miniaturized devices, the specific biorecognition elements are largely limited to enzymes, antibodies, aptamers, molecularly imprinted polymers (MIPs), *etc.* [11]. Among these biorecognition elements, enzymes have been widely used in biosensors including microfluidic systems due to their high reactivity, sensitivity, and specificity [12]. Researchers have developed typical immunoenzymatical assays based on the above features of enzymes. Horseradish

* Corresponding author. State Key Laboratory of Electroanalytical Chemistry, Changchun Institute of Applied Chemistry, Chinese Academy of Sciences, Changchun, Jilin, 130022, China.
** Corresponding author. College of Engineering and Applied Sciences, Nanjing National Laboratory of Microstructures, Jiangsu Key Laboratory of Artificial Functional Materials, Nanjing University, Nanjing, Jiangsu, 210023, China.
E-mail addresses: weihui@nju.edu.cn (H. Wei), duyan@ciac.ac.cn, duyan.bessie@gmail.com (Y. Du).

https://doi.org/10.1016/j.trac.2022.116858
0165-9936/

peroxidase (HRP), catalase (CAT), and alkaline phosphatase (ALP) are commonly used as enzymatic labels in classical enzyme linked immunosorbent assay (ELISA) [13–15]. They transduce the specific recognition into detectable quantitative signals. Benefiting from this excellent capacity, ELISA has become the "gold standard" surpassing other assays in lots of bioanalysis fields. Many comprehensive reviews about this assay have been summarized [16–20].

However, owing to the chemical structure of biological macromolecules, the inevitable disadvantages (low stability, high cost, and low tolerance to harsh environments) of enzymes have restricted their performance in many microfluidic bioanalysis conditions [21]. To overcome these shortcomings, the development of artificial enzymes has been demonstrated as a promising strategy [22]. Among the diverse candidates for artificial enzymes, nanomaterials with enzyme-like activities have been considered as the next generation of artificial enzymes [23–27]. In 2007, Gao et al. found that iron oxide nanoparticles (Fe_3O_4 NPs) possessed intrinsic peroxidase-like activity [23]. Numerous nanomaterials were subsequently proved to have the potential to play the same role as enzymes in many aspects. In 2013, Wei and Wang summarized these phenomena and formally defined nanozymes as the nanomaterials with enzyme-like characteristics [24]. Since then, nanozymes have been intensively employed in various disease management, such as inflammation alleviation, sepsis treatment, and tumor therapy [28–30]. Meanwhile, they have also been used in bioanalysis as the alternatives for enzymes, especially HRP, due to their advantages of high stability, low cost, and high robustness over enzymes. For example, a Fe–N–C nanozyme was applied in drug-drug interaction evaluation via both the accelerated and inhibited biocatalytic activities [31]. Numerous excellent studies have used nanozymes as the bioreceptors or signal transduction units [32–34]. By combining with microfluidic systems, nanozymes showed great promise in ion detection, biomolecular recognition, infections diagnosis and tumor monitoring in a simple, rapid, and portable approach [35–40]. For instance, an ultrasensitive microfluidic paper-based sensing platform toward miRNA could be achieved by ceria (CeO_2) nanozyme [37]. A well-designed convergence-divergence spiral microfluidic device could be used to achieve rapid and sensitive detection for *Salmonella* based on manganese dioxide (MnO_2) nanozyme [41].

In this review, we summarized the recent advances in microfluidic bioanalysis using nanozymes. First, we will introduce representative nanozymes used in microfluidic bioanalysis according to enzyme-like activity. Then, to achieve more sensitive and specific detection, we will focus on the cascade reaction coupling enzyme and nanozyme cascaded systems. Meanwhile, the improved selectivity by cascaded nanozymes in microfluidics will be discussed. Finally, the challenges and future directions are proposed to stimulate more researchers to make greater progress in this field.

2. Classification and typical nanozymes used in microfluidic bioanalysis

Since the unexpected intrinsic peroxidase-like activity of Fe_3O_4 NPs has been found, numerous nanomaterials were subsequently proved to possess intrinsic enzyme-like activity and were termed as nanozymes [23,24]. Besides peroxidase, diverse enzymes can be mimicked by nanozymes, including oxidase, catalase, superoxide dismutase (SOD), hydrolase, *etc*. Many analytical applications have been performed based on nanozymes [21,32]. Herein, we will discuss the representative microfluidic bioanalysis according to the activity of nanozymes.

2.1. Nanozymes with peroxidase-like activity

The nanozymes with peroxidase-like activity could catalytically oxidize some enzymatic substrates to their corresponding oxidized products under the assistance of peroxides especially hydrogen peroxide (H_2O_2) (Fig. 1a) [24,25]. Taking typical Fe_3O_4 NPs as an example, during the catalytic process, H_2O_2 was chemisorbed onto the surface to form two hydroxyl adsorbates, which served as an intermediate to oxidize chromogenic products [42,43]. For Prussian blue (PB) NPs, $^{\bullet}OH$ was not involved in the catalytic process. They served as electron transporters from electron donor to electron acceptor (*e.g.,* H_2O_2) [44]. The corresponding products could generate colorimetric, fluorescence, chemiluminescence or electric signals to indicate the presence of analytes in determined samples [32]. This property made peroxidase-like nanozymes as excellent signal translating modules. Therefore, they could be advanced to detect hydrogen peroxide or various metabolites and used as labels in immunoassay to replace HRP [21].

Based on the advantages of nanozymes over enzymes, conventional ELISAs using enzyme labels could be improved. A few proposals were made to improve the assay and a biomimetic nanozyme-linked immunosorbent assay (NLISA) was developed by replacing enzyme labels with nanozymes with peroxidase-like activity [47–49]. As shown in Fig. 1b, Xi et al. reported a type of nickel-platinum nanoparticles (Ni–Pt NPs) with ultrahigh peroxidase-like activity by rational design [45]. Additionally, the detection of carcinoembryonic antigen (CEA) was realized by a Ni–Pt NP-based immunoassay (Ni–Pt ELISA). During the detection process, the colorless substrate 3,3′,5,5′-tetramethylbenzidine (TMB) was converted into blue or yellow, which was stopped by H_2SO_4, like in a classical ELISA. The detection limit of developed Ni–Pt ELISA for CEA was as ultralow as 1.1 pg/mL, which was lower than that of traditional ELISA bioassays. The Ni–Pt ELISA showed that nanozymes could not only replace the role of enzymes, but also even perform better under certain conditions.

When peroxidase-like nanozymes were applied in microfluidic platforms, they were usually integrated into both electrochemical and colorimetric systems, acting as a peroxidase for signal transduction and amplification [37]. Due to the precise sample manipulating and controlling capability, microfluidics could be used to realize fluid handling, automation, and sample preparation. As illustrated in Fig. 1c, integrating the advantages of microfluidics and nanozymes, Liu et al. established this kind of dual-mode (electrochemical/visual) microfluidic device to determine circulating tumor cells (CTCs) in pheochromocytoma (PCC) rapidly and sensitively [46]. The automated sample separation, labeling, and detection were realized by a well-designed microfluidic chip combined with a signal analysis software on a smartphone. The electrochemical sensing signals were generated from the catalytical reduction of H_2O_2 by covalent organic framework based nanozymes (COF@Pt) in the presence of TMB. Meantime, the blue color of oxidized TMB could also reflect the level of PCC-CTCs. Under the collaboration of nanozyme and microfluidic system, a low detection limit of 1 cell/mL with a wide linear range of 2 to 10^5 cells/mL was realized. This study showed that nanozyme bioanalysis had unique characteristics, benefiting from the powerful microfluidic device.

Lateral flow immunochromatographic test strips, also referred to as lateral flow assays (LFAs), which based on colloidal NPs have been widely used in commercial point-of-care (POC) diagnosis method owing to their unique advantages (rapid speed, robustness, and ease-to-use) [9]. Colloidal NPs (gold, silver, selenium, *etc.*) usually served as signal reporters because of their unique optical (colorimetric, fluorescence, and chemiluminescence) or other (magnetic and surface-enhanced Raman scattering) properties

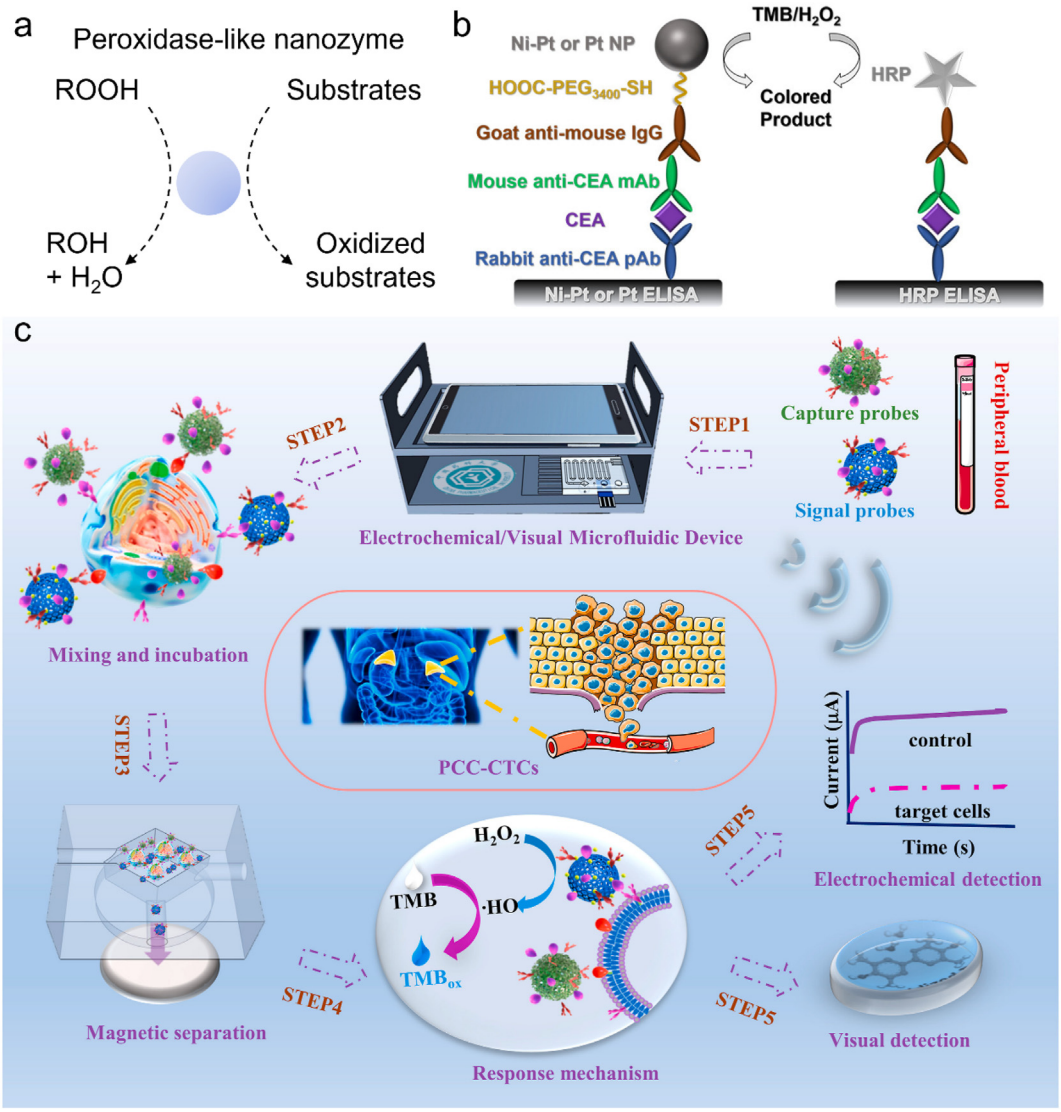

Fig. 1. Microfluidic bioanalysis based on peroxidase-like nanozymes. (a) Reaction catalyzed by peroxidase-like nanozymes. (b) Schematic of the Ni–Pt, Pt and HRP ELISA for CEA detection. (Reprinted with permission from Ref. [45]. Copyright (2021) American Chemical Society) (c) Schematic of electrochemical/visual microfluidic detection with a covalent organic framework supported platinum nanozyme-based device for early diagnosis of pheochromocytoma. (Reprinted with permission from Ref. [46]. Copyright (2022) Elsevier.).

[50]. These signal transduction processes could also be achieved using nanozymes and several important analytes (antibiotic, bacterias, viruses, *etc.*) were successfully detected in a more rapid, more sensitive, and simpler measure via nanozyme based strip (nanozyme-strip) [51–55]. Currently, the global coronavirus disease 2019 (COVID-19) pandemic caused by the novel coronavirus SARS-CoV-2 could be effectively controlled by early and rapid detection techniques [56,57]. As shown in Fig. 2a, Liu et al. demonstrated a Co–Fe@hemin nanozyme-strip using luminol as a chemiluminescence substrate, which could detect recombinant spike antigen (S-RBD) of SARS-CoV-2 [58]. The strip was constructed on the mechanism of traditional double antibody sandwich LFA. Generally, once the lateral flow of the sample solution containing S-RBD contacted with the preloaded Co–Fe@hemin nanozyme labeled with S-dAb (detection antibody of S-RBD) and S-cAb (capture antibody of S-RBD), the sandwich immunocomplexes would form. A chemiluminescence signal would generate upon the subsequent addition of H_2O_2 and luminol due to the high peroxidase-like activity of nanozyme. The nanozyme-strip could achieve a linear range of 0.2–100 ng/mL and a detection limit of 0.1 ng/mL (Fig. 2b and c).

In addition, the bacterial infections have received more and more attention due to the emergence of bacterial multidrug resistance [59]. Therefore, the sensitive detection methods of bacteria are on greatly demanded and nanozymes have been explored in this field [60,61]. A sensitive and simple nanozyme-strip developed by Cheng et al. showed great potential owing to the high performance of Pd@Pt nanozyme and the convenience of LFA paper-based microfluidics [52]. The nanozyme-strip was also advanced to monitor important biomarkers by the same group [54]. In this study, total butyrylcholinesterase (BChE) was detected based on the peroxidase-like PtPd nanozyme, showing the versatility of nanozyme based paper microfluidics. Moreover, it not only suggested that nanozyme-strip had potential wide range of applications as a universal low-cost paper-based microfluidic platform, but also illustrated that the nanozyme could also be used as an applicable, robust, versatile, and universal signal transduction module beyond artificial enzyme mimics in microfluidic systems.

Other than replacing natural peroxidase to serve as a reporter, the analytical applications based on nanozymes have attracted

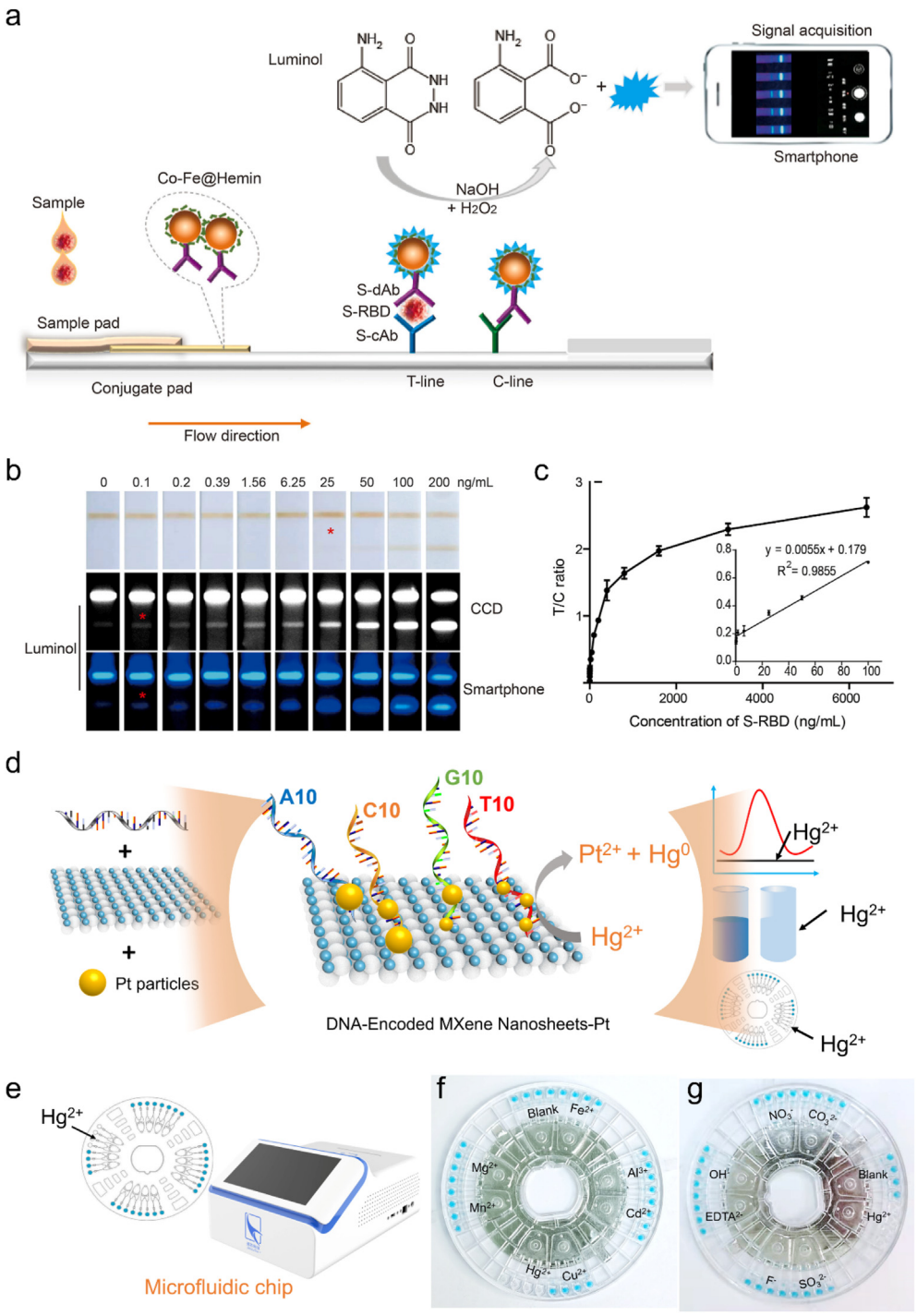

Fig. 2. Microfluidic bioanalysis based on peroxidase-like nanozymes. (a) Schematic of the nanozyme chemiluminescence paper test for SARS-CoV-2 S-RBD antigen. (b) Gradient paper testing of SARS-CoV-2 S-RBD protein before and after adding luminol and (c) the corresponding calibration curve. (Reprinted with permission from Ref. [58]. Copyright (2021) Elsevier.) (d) Schematic of DNA-encoded MXene-Pt nanozyme for enhanced colorimetric sensing of Hg^{2+}. (e) Schematic of designed centrifugal disk-like microfluidic chip and the automated microfluidic chip detection system. (f and g) Photographs of color change in microfluidic chip after catalytic reaction with various metal ions (f) and anions (g). (d-g, reprinted with permission from Ref. [35]. Copyright (2022) Elsevier.).

more and more interest [33]. As an excellent example shown in Fig. 2d, Shi et al. enhanced the peroxidase-like activity of virginial transition metal carbide/nitride (MXene) by a simple DNA-encoded seed-growth strategy [35]. Meanwhile, a multimode (UV—vis spectrometer, naked eye, and microfluidic chip) sensing system for Hg^{2+} was developed because the boosted peroxidase-like activity of MXene/DNA/Pt nanozyme would be inhibited after the specific capture of Hg^{2+}. It was noted that the centrifugal disk-like microfluidic chip equipped with an automated microfluidic chip detection system was applied to realize the high-throughput screening for various samples (Fig. 2e). Simultaneously, microfluidics could minimize the sample requirement of potential toxic analytes. As the photographs shown in Fig. 2f and g, the diverse potential interfering anions and cations were tested at the same time, and only

Hg^{2+} could effectively inhibit the activity of as-prepared nanozyme. In addition, other analytes which would regulate nanozyme activity could also be successfully recognized in microfluidic devices.

In addition to these detection and diagnosis systems, the enzyme-free bioassays which integrate the peroxidase-like nanozymes and microfluidic systems have made great progress in bioanalysis [62–68]. For example, Sharafeldin et al. developed an electrochemical microfluidic platform toward cancer biomarker proteins based on the peroxidase-like Fe_3O_4@graphene oxide nanozyme [65]. Of note, other than the peroxidase-like activity, the magnetism of Fe_3O_4 was used to separate samples, suggesting the unique properties of nanozymes against enzymes. Additionally, Koo et al. demonstrated that the microfluidic chip could be used for specific target genes analysis using peroxidase-like nanozyme as a signal probe [67]. These works showed that, in the microfluidic bioanalysis area, peroxidase-like nanozymes could be used to replace natural HRP labels and the interaction between analytes and nanozymes could be used to set up microfluidic bioanalysis platforms, enabling nanozymes to be more than artificial enzyme mimics [69]. The peroxidase-like nanozyme bioanalysis could be more convenient, more rapid, and portable, by combining the advantages of microfluidic platforms.

2.2. Nanozymes with oxidase-like activity

Different from the peroxidase-like activity, the nanozyme with oxidase-like activity can catalyze the oxidation of a substrate to the corresponding oxidized product in the absence of H_2O_2, where molecular oxygen (O_2) serves as the electron acceptor (Fig. 3a) [70–73]. Typically, the activation of O_2 is the key step to impart nanozymes with oxidase-like activities [74]. For noble metal nanoparticles, such as gold, silver, and platinum, the single atom O derived from the dissociative adsorption of O_2 on the metal surfaces accounts for their oxidase-like activities [70]. For single-atom nanozymes, a series of reactive oxygen species (ROS), including superoxide radicals ($O_2^{\bullet-}$), singlet oxygen, and H_2O_2, would form during the catalytical process [75]. Besides the common substrates (TMB, ABTS and Amplex red), other substrates such as glucose, polyphenols, glutathione, and sulfite, were also explored [76–78]. And various kinds of nanozymes with oxidase-like activity have been exploited in biosensing [79–82]. For microfluidic technology, Tran et al. developed a paper-based microfluidic device that could determine diverse phenolic compounds by a facile way using DNA-copper hybrid nanoflowers (GNFs) with intrinsic laccase-like (polyphenol oxidase-like) activity (Fig. 3b) [83]. The laccase-like activity of GNFs was acquired via mimicking the active sites of natural laccase. In the wax-printed paper microfluidic device, GNFs could catalyze the oxidation of phenolic compounds to react with 4-aminoantipyrine (4-AP) to generate a color change for colorimetric detection. Three kinds of phenolic compounds (*i.e.*, dopamine, catechol, and hydroquinone) were demonstrated in the study. After the data analysis via smartphone, their detection limits were determined to be 4.5, 3.0, and 4.5 μg/mL, respectively. The device also exhibited long-term stability over 2 months, showing the advantage of the combination of nanozyme and microfluidics.

Beyond the paper-based microfluidic platform, as shown in Fig. 3c, Wu et al. prepared a cupric oxide (CuO) nanozyme with ascorbate oxidase-like activity and developed a dual-mode microfluidic sensing platform for ultrasensitive detection toward neuron specific enolase (NSE) [84]. In this study, the photoelectrochemical (PEC) signal generated from photoactive zinc oxide (ZnO) nanoflowers has been significantly enhanced by modified gold (Au) and silver antimony sulfide ($AgSbS_2$) nanoparticles, due to the localized surface plasmon resonance (LSPR) effect of Au and matching electronic band structure between ZnO and $AgSbS_2$. After the formation of sandwich structure of Antibody 1 labeled ZnO/Au/$AgSbS_2$, NSE and Antibody 2 labeled CuO nanozyme, the original signal would be quenched by the catalytic reaction of CuO nanozyme toward ascorbic acid (AA), meanwhile a fluorescent signal would be initiated during the process. Of note, ZnO nanoflowers used to produce PEC signal were also synthesized via a microfluidic reactor, suggesting that microfluidic chips could also be used to synthesize and engineer nanozymes, another aspect of microfluidics as a powerful synthesis platform [85].

Other than the nanozyme involving *in vitro* diagnostics (IVD) microfluidic techniques, an *in vivo* online electrochemical detection platform was advanced by Wang et al. [78]. As described in Fig. 3d, they presented an engineered metal-organic framework (MOF) with enhanced oxidase-like activity via a defect-tuning strategy. The main interference (AA, dopamine, and 3,4-dihydroxyphenylacetic acid) toward uric acid (UA) detection was depleted completely, based on the ascorbate oxidase- and laccase-like activity of developed nanozyme. After flowing through a microreactor pre-loaded with the oxidase-like nanozyme, the concentration of uric acid in rat brain was monitored successfully by the following online electrochemical system during the ischemia reperfusion injury. As shown in Fig. 3e, in the absence of microfluidic device containing oxidase-like nanozyme, the electrical signal would be generated with the addition of interfering substances. This problem was addressed with the aid of nanozyme (Fig. 3f). The UA level in striatum of living rats was consistent with other studies and the enhanced current caused by global ischemia would return to the normal level during the reperfusion. Lin group also developed an online microfluidic platform for hydrogen sulfide (H_2S) monitoring using laccase-like molybdenum doped PB analog nanozyme. The nanozyme would address the low stability issue of natural laccase that would be affected by the undesirable ions in cerebrospinal fluid (CSF) [86]. The laccase-like activity of engineered nanozyme would decrease after the etching of H_2S. Additionally, dopamine was used as the oxidase substrate instead of the commonly-used TMB to avoid the influence caused by potential reducibility of H_2S. Utilizing the similar microfluidic chip shown in Fig. 3d, the H_2S level in CSF was successfully monitored. Besides the oxidase-like activity could be used to report the H_2S level, the catalase- and peroxidase-like activity could scavenge the radicals in cells to realize the cytoprotective effect.

In the section of oxidase-like nanozymes involved in microfluidic bioanalysis, the nanozymes could not only be used as novel signal transduction unit but also had merits in producing or removing signals based on the oxidase-like activity via the precisely controlled manipulation of microfluidics. The designed microfluidic devices based on oxidase-like nanozyme could greatly extend the scope of bioanalysis because of the various substrates. The relationship between oxidase-like nanozyme and substrates could provide more novel sensing strategies and inspire more possibilities in the future.

2.3. Nanozymes with catalase-like activity

The excess H_2O_2 in organisms that would cause serious oxidative damage could be degraded into H_2O and O_2 efficiently by catalase and its mimics (Fig. 4a) [87–90]. For noble metal nanoparticles, under basic conditions, the acid-like decomposition of H_2O_2 on the metal surfaces would generate adsorbed H (H*) and HO_2 (HO_2*). Subsequently, the HO_2* would transfer a H atom to another H_2O_2* molecule, yielding an O_2* and converting the H_2O_2* to H_2O* and OH* [91]. The catalase-like nanozymes could not only be used for tumor hypoxia suppression, inflammation improvement, and neurodegenerative disease but also could act as an excellent bridge connecting nanozymes and microfluidics owing to

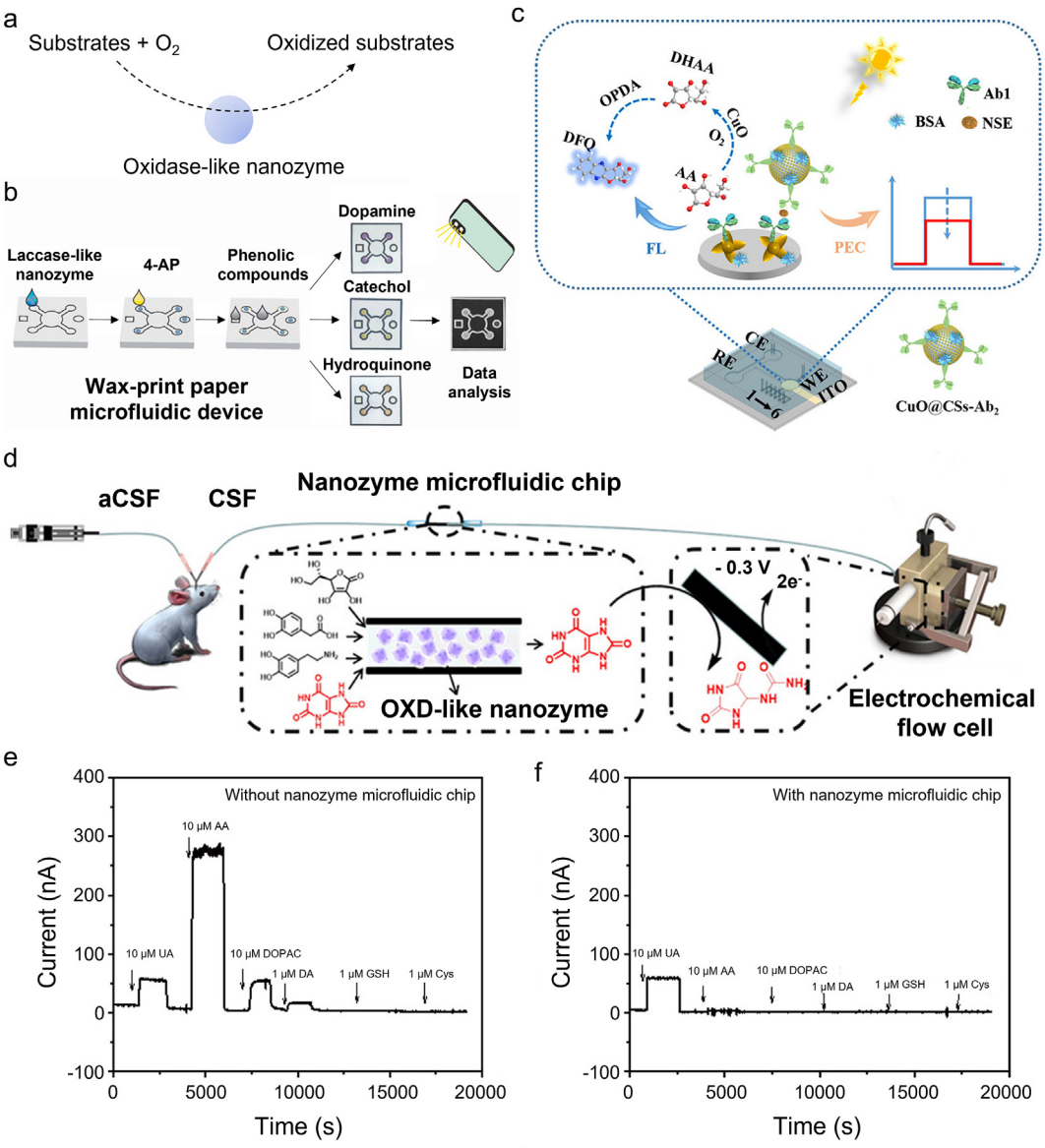

Fig. 3. Microfluidic bioanalysis based on oxidase-like nanozymes. (a) Reaction catalyzed by oxidase-like nanozymes. (b) Schematic of DNA-copper hybrid nanoflowers as efficient laccase-like nanozymes for colorimetric detection toward phenolic compounds. (Reprinted with permission from Ref. [83]. Copyright (2021) Elsevier.) (c) CuO nanozymes as multifunctional signal labels for construction of a dual-mode microfluidic sensing platform. (Reprinted with permission from Ref. [84]. Copyright (2022) American Chemical Society.) (d) Schematic of an MOF nanozyme regulatory strategy based on selective online electrochemical analysis of uric acid. Typical current signal recorded for UA and other interfering substances in the online system in the absence (e) or presence (f) of nanozyme microfluidic chip. (d-f, reprinted with permission from Ref. [78]. Copyright (2021) American Chemical Society.).

the produced gas in the channels of microfluidic chips [92–94]. As shown in Fig. 4b, Song et al. developed a quantitative DNA detection assay using a visual multistage propelled volumetric bar chart chip (V-Chip) [95]. To detect the target DNA sequence, a classical sandwich DNA hybridization principle was applied in the assay. Commonly, a designed captured DNA strand was modified onto the assay wells before the detection assay. Following the addition of target sequence solution, the probe DNA labeled catalase was loaded into the microchannel to initiate the propellant reaction. The deposited Pt nanozyme was employed to produce the signal. Like the work catalyzed by catalase, Pt nanozyme with catalase-like activity could decompose H_2O_2 to produce O_2, pushing the subsequent preloaded red ink in chip channels to realize visual detection during the signal amplification process [96]. By this amplification strategy, DNA as low as 20 pM could be easily detected. More importantly, the distance ink traveled could be read by naked eyes directly. The fully utilized microfluid manipulation reflected the unique advantages of the integration of microfluidic technology and nanozymes. This powerful microfluidic chip was improved by introducing a target-responsive hydrogel embedding a catalase-like Au@Pt nanozyme by Zhu et al. [97]. Upon meeting the target, the hydrogel would rapidly decompose and the released Au@Pt nanozyme could produce enough O_2 to drive the ink in the V-Chip. To avoid the limitations of catalase, a catalase-like nanozyme was used as the sole signal amplification unit. And the developed target-responsive hydrogel could be designed to recognize other substances. The universal POC detection platform could be expanded by changing the corresponding recognition element. It is believed that this power-free and portable POC microfluidic chip would make great contributions in undeveloped areas.

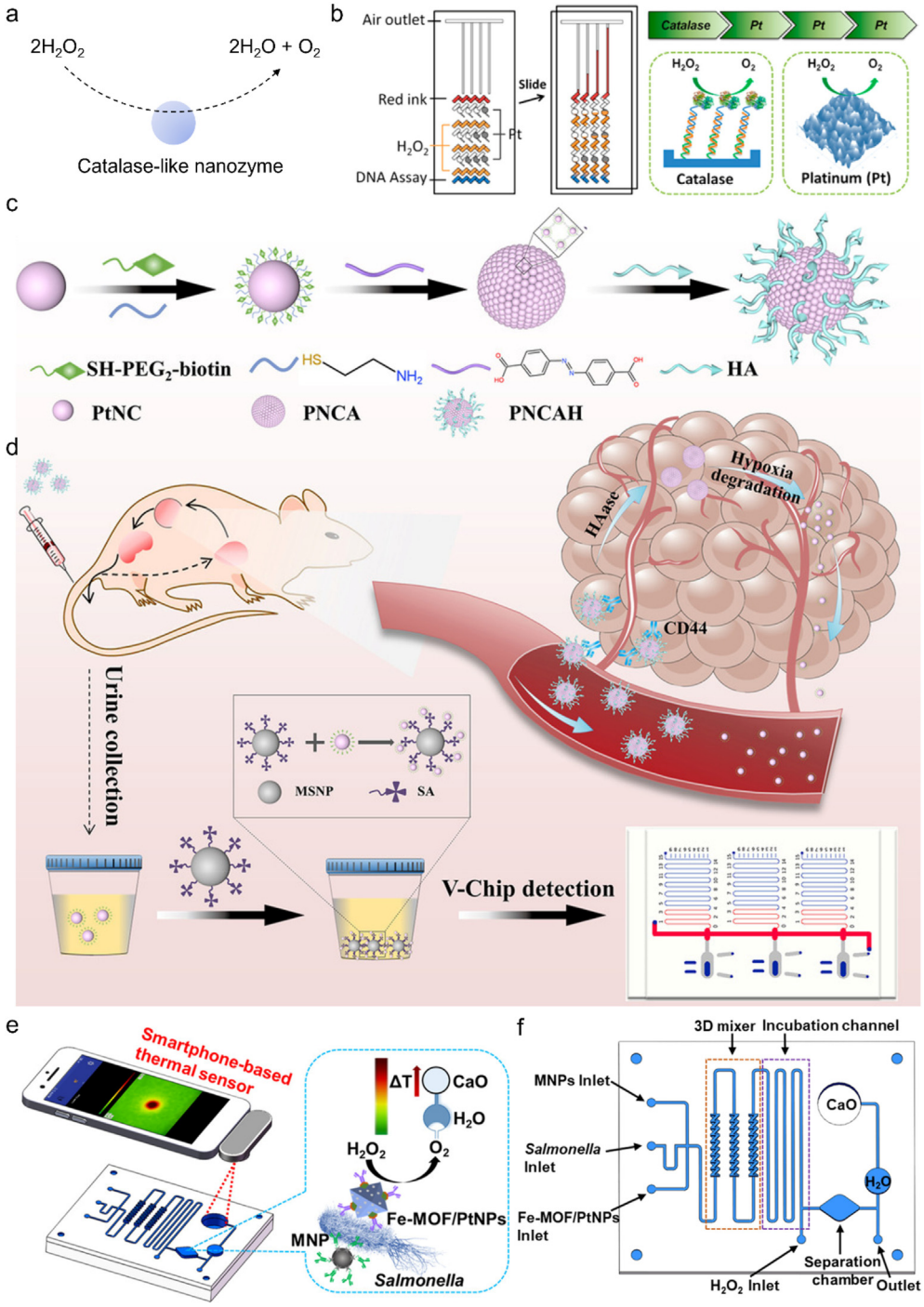

Fig. 4. Microfluidic bioanalysis based on catalase-like nanozymes. (a) Reaction catalyzed by catalase-like nanozymes. (b) Schematic of the multistage V-Chip for visualized quantification of DNA. (Reprinted with permission from Ref. [95]. Copyright (2013) American Chemical Society.) (c) Preparation process of Pt supernanoparticles. (d) Schematic of hypoxia-responsive Pt supernanoparticles for urinary microfluidic monitoring of tumors using a V-Chip. (c and d, reprinted with permission from Ref. [40]. Copyright (2022) John Wiley and Sons.) (e) Schematic of MOF nanocubes decorated with Pt nanozyme for the detection of *Salmonella* and designed microfluidic chip (f). (e and f, reprinted with permission from Ref. [98]. Copyright (2021) American Chemical Society.).

Afterwards, a wide range of analytes were successfully determined by this principle via catalase-like nanozymes [38,40,99–109]. Among them, Xu et al. synthesized hypoxia-sensitive platinum supernanoparticles (PNCAH) which would be dissociated into catalase-like Pt nanozymes after the response to a hypoxic microenvironment, an important prognostic factor in many kinds of cancer (Fig. 4c). [40]. As shown in Fig. 4d, the noninvasive detection of the triple-negative breast cancer (TNBC) and its lung metastasis was carried out by the Pt nanozyme filtered through the kidney and the following V-Chip. For tumor detection *in vivo*, TNBC model and healthy mice were injected with PNCAHs. After the hypoxia-responsive degradation of PNCAHs, urine was collected from different mice. Compared to the healthy group, the model group showed a significant signal increase, which could be

read by V-Chip, suggesting the ability of PNCAHs to monitor disease. Furthermore, the healing process of paclitaxel, a kind of typical antitumor drug, in TNBC mice was observed on the V-chip. Moreover, this simple, portable, and noninvasive microfluidic chip could be adapted to perform a universal diagnostic platform by replacing corresponding specific recognition elements.

Though the signal transduction strategy in which an ink is pushed by the generated gas has been constantly improved, other effective strategies were also proposed. As shown in Fig. 4e, Guo et al. designed a microfluidic biosensing platform based on the heat produced from the reaction between H_2O and calcium oxide (CaO) powder [98]. In the process of detection, the immune peroxidase-like Fe-MOF/Pt nanozyme, bacterial analytes to be determined, and antibody labeled magnetic nanoparticles (MNPs) flowed through three channels, respectively (Fig. 4f). After mixing in the three-dimensional (3D) mixer, they would form the MNPs-bacteria-Fe-MOF/Pt nanozyme sandwich structure. Then, with the addition of H_2O_2, the preloaded H_2O in channels would be pushed into the heating chamber containing CaO by the pressure produced from the catalase-like nanozyme catalysis. The detection limit for *Salmonella* was as low as 93 CFU/mL within 1 h by using the Fe-MOF/Pt nanozyme. Importantly, a 3D chaotic micromixer was used for automatic operations, suggesting that the versatile microfluidic device could enhance the sensing efficiency and achieve more accurate results. Besides these strategies, other POC biosensing devices were also constructed using catalase-like nanozymes [110–113]. For example, Zhu et al. used the pressure change caused by catalase-like nanozyme to realize the immunodetection for prostate specific antigen (PSA) using a handheld pressure meter [111]. Furthermore, Yu et al., reported the POC detection using a similar strategy with a commercial digital multimeter [112]. The flexible pressure sensor was mediated by the multiwalled carbon nanotube-decorated paper. Overall, as the decomposition products of H_2O_2 catalyzed by catalase-like nanozyme, both H_2O and O_2 could be used to generate visual signals in microchannels of microfluidic devices. It was believed that more and more interesting applications would be explored by using catalase-like nanozymes in microfluidics.

2.4. Nanozymes with superoxide dismutase (SOD)-like activity

SOD is a collection of important antioxidant enzymes which can regulate oxidative stress levels *in vivo* by catalyzing the dismutation of $O_2^{\bullet-}$ into H_2O_2 and O_2 (Fig. 5a) [114]. For this kind of nanozymes, Wang et al. found that the catalytic mechanism depends on the electron occupancy in intermediate frontier molecular orbital (iFMO) of nanozyme by theoretical calculation. The reaction follows a lowest unoccupied molecular orbitals (LUMO)-mediated mechanism when the iFMO of nanozyme is unoccupied FMO. Typically, one $O_2^{\bullet-}$ would be first oxidized to O_2 by nanozyme, and then the reduced nanozyme would be oxidized by another $O_2^{\bullet-}$, with the generation of H_2O_2. In contrast, the mechanism follows a highest occupied molecular orbitals (HOMO)-mediated type when the iFMO of nanozymes is occupied FMO. $O_2^{\bullet-}$ would be first reduced to H_2O_2 by nanozyme and then the oxidized nanozyme would be reduced by another $O_2^{\bullet-}$, with the production of O_2. When the iFMOs are both occupied and unoccupied FMOs, both mechanisms work together [115]. Like the catalase-like nanozymes, departing from being used to treat various diseases, the SOD-like nanozymes could also be applied to develop biosensors toward $O_2^{\bullet-}$ released from living cells [116–119]. Natural SOD could be used in the electrochemical determination of $O_2^{\bullet-}$ owing to the specific molecular recognition for $O_2^{\bullet-}$ [120]. Inspired by this, the sensing strategy was proved effective by replacing the SOD with SOD-like nanozymes [116–119]. Commonly, a sensitive electrochemical method was also employed to construct *in-situ* biosensors toward $O_2^{\bullet-}$ using nanozymes. Therefore, biocompatibility of nanozyme modified electrodes should be considered, because the living cells directly adhered and grew on the surface of electrodes.

By combining the previous microfluidic chip fabrication technology (Fig. 5b), Wang et al. successfully developed a sensitive (1.6 μA/μM) and specific electrochemical detection system using the SOD-like nano-$Mn_3(PO_4)_2$-chitosan nanozyme from murine breast tumor cells (4T1) lines (Fig. 5c) [119,121]. The detection limit was as low as 9.4 nM, which was more sensitive than the classical electron paramagnetic resonance (EPR). As shown in Fig. 5d, Bao group also constructed an *in-situ* real-time $O_2^{\bullet-}$ monitoring platform from living cells using a highly biosafe bacterial cellulose@DNA-$Mn_3(PO_4)_2$ nanozyme [122]. During the detection process, once the $O_2^{\bullet-}$ was released from the human breast cancer cell line (MCF-7) and lung carcinoma epithelial cell (A549) lines, the specific current signal would be generated. Since no obvious signal appeared upon the addition of interference, it suggested the good selectivity of BC@DNA-$Mn_3(PO_4)_2$ toward $O_2^{\bullet-}$ (Fig. 5e). From Fig. 5f and g, one could observe the apparent quick stepwise current signals with the elevated $O_2^{\bullet-}$ concentration. A linear range from 34.7 nM to 7 μM with a detection limit of 5.87 nM was obtained. In both studies, the microfluidic channel provided a facile approach for samples going through toward the detector area, which greatly decreased the sample requirement, showing the advantages of microfluidic chips. With the development of nanozymes, it was expected that more SOD-like nanozymes could be used to construct biosensors and more sensing principles using microfluidics would be developed other than the current strategies.

3. Microfluidic bioanalysis based on cascaded systems

Since the enzymes have specificity towards distinct reactions, the collaboration of multiple enzymes was required in some intricate conditions by concurrent or sequential approaches [123–125]. The multienzyme cascade reaction systems could be used to realize various applications which could not be reached by individual enzyme [124]. Multienzyme cascade reactions were also applied to construct biosensors in microfluidic channels [126].

3.1. Cascade system by enzymes

Like the natural counterparts, though nanozymes have been widely used as the signal reporters in bioanalysis, the individual catalytic process still greatly limits the further development of nanozyme bioanalysis [34,127]. Therefore, like multienzyme cascade reaction, the combination of nanozymes or other artificial enzyme mimics with enzymes would further widen the repertoire of bioanalysis [123]. Wei and Wang provided a strategy to couple a Fe_3O_4 nanozyme with glucose oxidase (GOx) that could broaden the scope of nanozyme biosensing [128]. By combining with enzymes, the specific and sensitive detection could be achieved due to the high efficiency of enzymatic catalysis in microfluidic devices [129–131]. As shown in Fig. 6a, the produced H_2O_2 from the oxidation of substrate 1 catalyzed by an oxidase could act as the substrate in the later reaction catalyzed by a nanozyme. Similarly, the role of an oxidase in cascade reaction could also be substituted by a nanozyme with oxidase-like activity (Fig. 6b).

As described in Fig. 6c, Nguyen et al. rationally developed a Co-doped mesoporous cerium oxide (Co-m-ceria) nanozyme with superior peroxidase-like activity at a neutral pH with a higher H_2O_2 adsorption capacity and easier H_2O desorption compared to pristine m-ceria [132]. The optimized Co-m-ceria nanozyme was used to construct cascaded biosensors using a paper microfluidic device toward five kinds of biomarkers by loading their corresponding

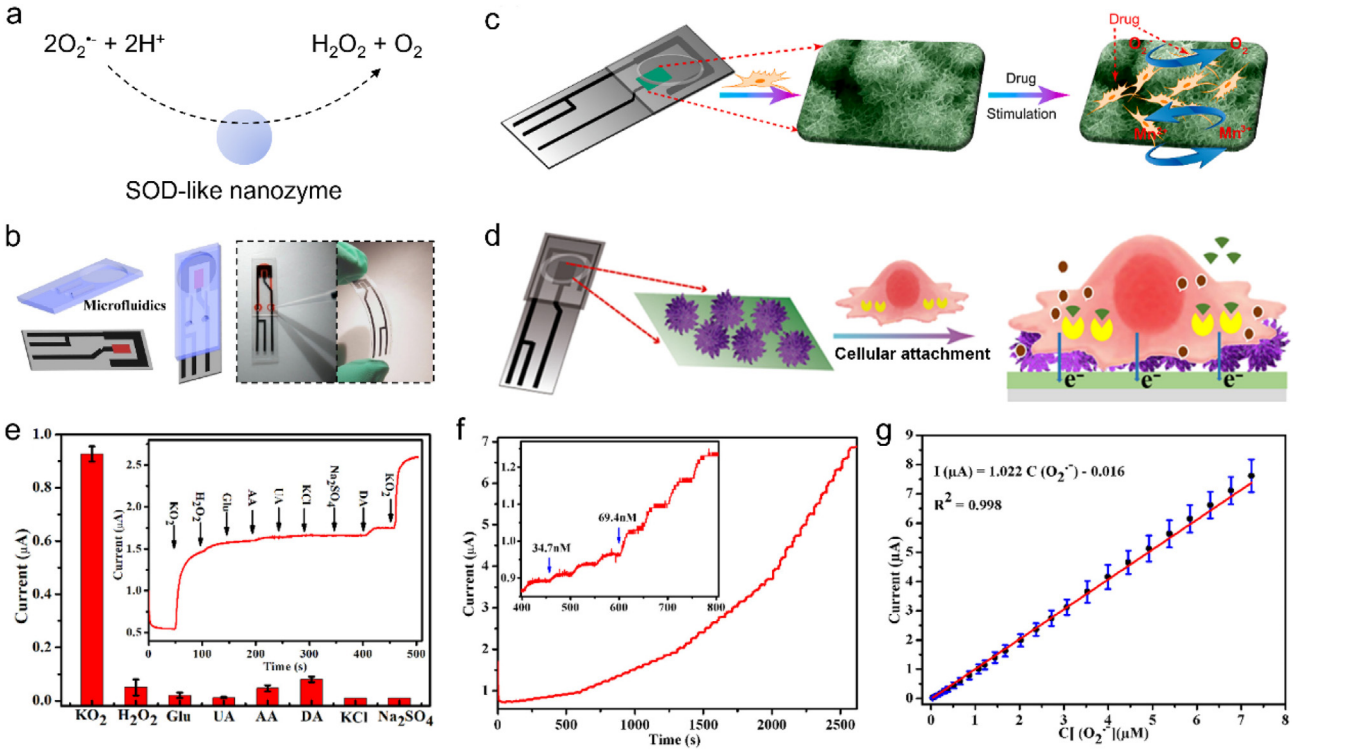

Fig. 5. Microfluidic bioanalysis based on SOD-like nanozymes. (a) Reaction catalyzed by SOD-like nanozymes. (b) Schematic of microfluidic package process and the optical photographs. (Reprinted with permission from Ref. [121]. Copyright (2017) Elsevier.) (c) Schematic of nano-$Mn_3(PO_4)_2$-chitosan *in situ* electrochemical detection interface for superoxide anions released from living cells. (Reprinted with permission from Ref. [119]. Copyright (2019) Elsevier.) (d) Schematic of BC@DNA-$Mn_3(PO_4)_2$ nanozyme for real-time monitoring of superoxide from living cells. (e) Selective performance of BC@DNA-$Mn_3(PO_4)_2$, (f) chronoamperometric response and (g) linear calibration curve of BC@DNA-$Mn_3(PO_4)_2$ sensors upon continuous addition of different concentrations of $O_2^{\bullet-}$. (d-g, reprinted with permission from Ref. [122]. Copyright (2020) American Chemical Society.).

oxidative enzymes into the pores. Upon the addition of target analyte, the oxidase would convert the substrate to its oxidation state and H_2O_2, which could serve as the substrate of the following colorimetric reaction. The developed colorimeter paper microfluidic device, which incorporated oxidase@Co-m-ceria enabled convenient and simultaneous detection of multiple biomarkers. The selective, sensitive, and immediate determination for glucose, galactose, cholesterol, choline, and acetylcholine were realized on paper-based microfluidic devices owing to the integrated oxidases. This study fully utilized the advantages of microfluidics and cascade nanozymes to realize simple and instant POC detection.

The unique and precise microdroplets transfer capability of microfluidic chip endowed cascaded nanozymes play excellent role in bioanalysis. As shown in Fig. 6d, Cheng et al. reported an *in vivo* analytical system [133]. They designed an integrated nanozyme by simultaneously loading GOx and hemin into the zeolitic imidazolate framework (ZIF-8). The outstanding sensitivity and selectivity for glucose were obtained because of the proximity effect at nanoscale and GOx in the cascade reaction. Furthermore, facilitated with microdialysis and microfluidic technology, the real-time online glucose level in the brains of living rats monitoring system was successfully constructed. Before the detection process, the well-designed nanozymes were pre-fixed onto the channels of the microfluidic chip. The dialysates from rat brain were continuously pumped to the nanozyme immobilized microfluidic chip, along with the fluorescent substrate Ampliflu Red. The fluorescent signal would be generated upon the cascade reaction occurred. Continuous and sensitive monitoring was achieved by this platform. Importantly, diverse biomarkers in *in vivo* monitoring platform could be achieved just by changing the oxidase in cascaded nanozymes benefiting from the natural enzyme involved.

In the paper-based and online analytical platform mentioned above [132,133], in the presence of specific substrates, the oxidases could convert them into H_2O_2 and trigger the subsequent reaction. The cascade reaction could be used to determine the substrate of oxidase. Practically, the specific reaction relationship could also be used to detect or evaluate the activity of enzymes [80,135]. Liu et al. proposed a microfluidic device to monitor the health status of liver by three relevant indicators: aspartate transaminase (AST), alanine transaminase (ALT), and alkaline phosphatase (ALP) (Fig. 6e) [134]. The different reaction substrates and peroxidase-like nanozymes were embedded into the agarose hydrogel. Upon introducing AST and ALT, the individual cascade reaction would take place and the TMB based colorimetric process would describe the produced results. ALP could catalytically convert ascorbic acid 2-phosphate to AA, which could discolor the blue oxidized TMB to perform a signal-off detection [136]. Under the cooperation of microfluidics and smartphones, the color information could be translated into digital signals, which realized synchronous quantitative evaluation of ALT, AST, and ALP with detection limits of 15, 10, and 5 U/L, respectively. In addition, the disposable hydrogels in the microfluidic chip could be replaced by the new ones for the subsequent detection.

Benefiting from the unique properties of enzymes, diverse analytes could be detected sensitively and selectively utilizing the cascade reaction under the collaboration of natural oxidases and peroxidase-like nanozymes. And the enzymes could be evaluated in turn using the corresponding substrates. Furthermore, the flow of droplets in microfluidics could be easily used to build reaction in sequence. The product of the first reaction could be easily brought into the subsequent chamber to start the following reaction, suggesting the advantage of microfluidics to build cascade reactions.

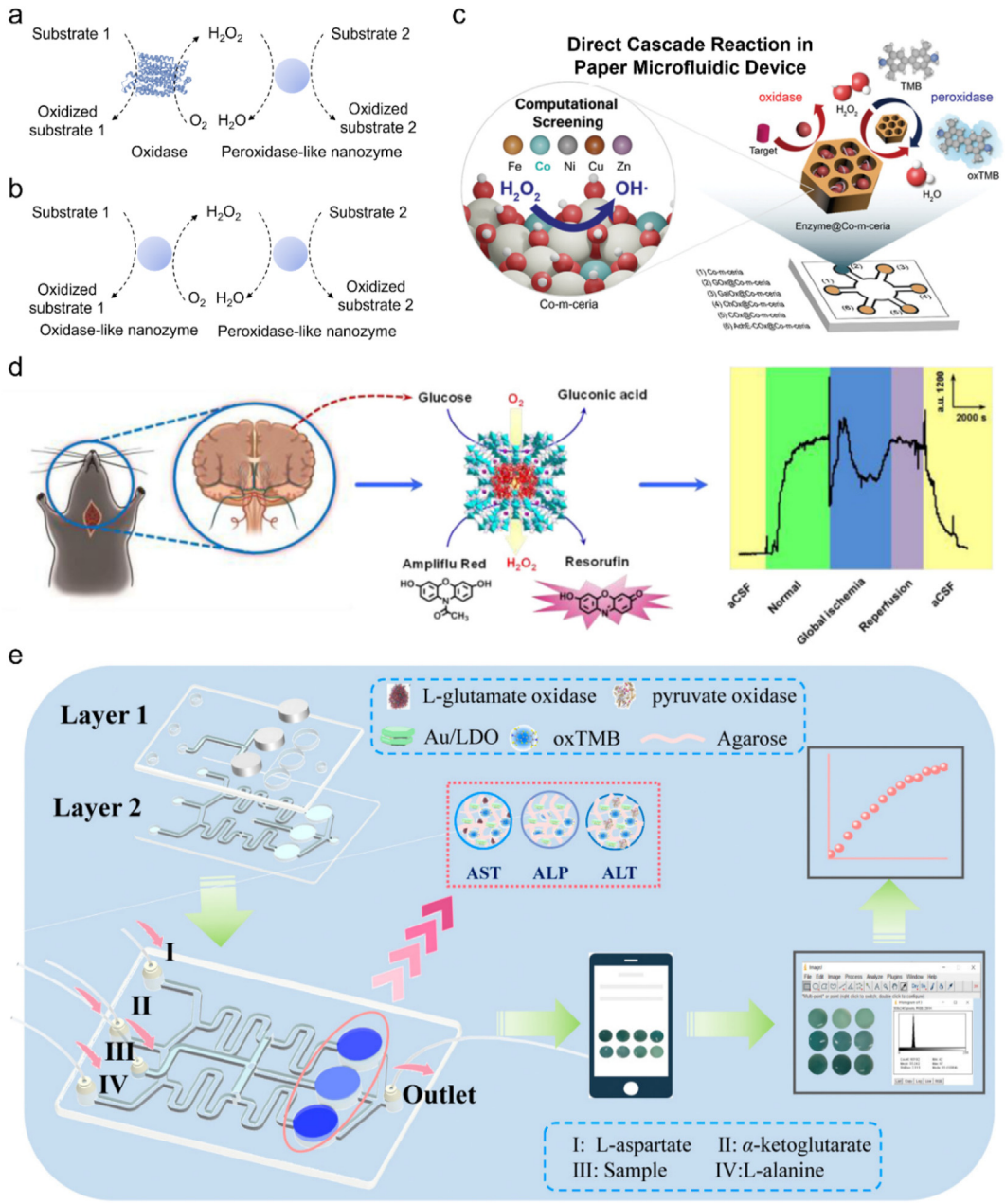

Fig. 6. Microfluidic bioanalysis based on cascade system. (a) Cascade system involving enzymes and (b) cascaded nanozyme system. (c) Schematic of the rational development of Co-m-ceria, which exhibits high peroxidase-like activity under a neutral pH, and its application in a paper microfluidic device for the quantitative determination of several biomarkers. (Reprinted with permission from Ref. [132]. Copyright (2022) John Wiley and Sons.) (d) Schematic of integrated nanozymes with nanoscale proximity for *in vivo* neurochemical monitoring in living brains. (Reprinted with permission from Ref. [133]. Copyright (2016) American Chemical Society.) (e) Schematic of hydrogel-involved colorimetric platforms based on layered double oxide nanozymes for POC detection of liver-related biomarkers. (Reprinted with permission from Ref. [134]. Copyright (2022) American Chemical Society.).

Overall, the cascade strategy between enzymes and nanozymes not only made it possible to perform selective and sensitive bioanalysis in microfluidics but also improved the stability compared to multienzyme cascade reactions [34].

3.2. Cascade system by nanozymes

Though the cascade reaction catalyzed by the combination of enzyme/nanozyme has achieved great progress, the shortcomings of enzymes still exist in such hybrid cascade systems. To minimize the use of enzymes, researchers designed the nanozyme-nanozyme cascade system, which did not involve enzymes (Fig. 6b) [137–139].

For example, Zhang et al. found that the K^+ modified graphitic carbon nitride (AKCN) exhibited oxidase- and peroxidase-like activities at the same time (Fig. 7a) [140]. As illustrated in Fig. 7b, the designed microfluidic chip provided a platform to perform sequential reactions. During the catalysis of AKCN (GOx-activity) under visible light, O_2 would be continuously purged in the oxidation process of glucose, and the produced H_2O_2 would be brought into the following channel and serve as the substrate in the subsequent reaction (still catalyzed by AKCN with the peroxidase-like activity) in the reactive chamber. Under the teamwork of microfluidic technology and multienzyme-like AKCN, a real-time POC biosensor toward glucose was developed. The initial reaction

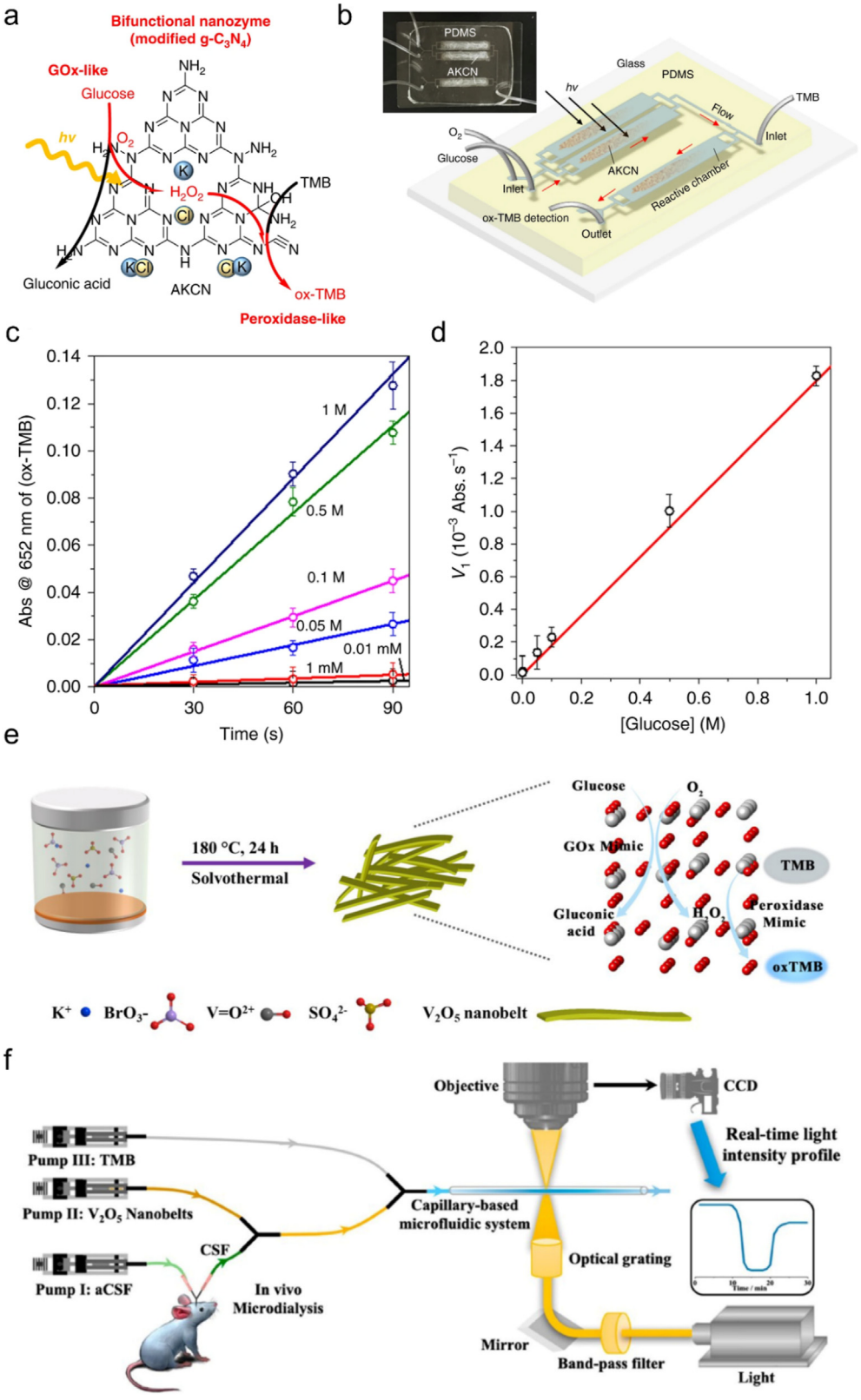

Fig. 7. Microfluidic bioanalysis based on cascaded nanozymes. (a) Schematic of glucose detection using a self-cascade nanozyme. (b) Schematic of the cascade reaction in a microfluidic device and actual device image (inset). (c) Kinetic curves of TMB oxidation in the microfluidic channel for glucose detection and (d) corresponding linear calibration. (a-d, reprinted with permission from Ref. [140]. Copyright (2022) Springer Nature.) (e) Synthesis process of self-cascade V_2O_5 nanozyme. (f) Online optical detection platform obtained by directly integrating a visible light absorption-based probe generated by the self-cascade catalysis. (e and f, reprinted with permission from Refs. [32,141]. Copyright (2020 and 2022) American Chemical Society.).

rate could be conducted from the kinetic curves of oxidized TMB (Fig. 7c). Combining the linear calibration in Fig. 7d, a low detection limit of 0.8 μM within 30 s would be realized. This study showed that the enzyme-free sensing system could be established completely by nanozymes.

Beyond the nanozyme-nanozyme cascade systems, the nanozyme with multienzyme-like activities could be used to develop self-cascade sensing system [142,143]. To achieve the continuous monitoring of glucose solely using a self-cascade nanozyme, Ding et al. prepared a vanadium pentoxide (V_2O_5) nanozyme that possessed both GOx- and peroxidase-like activities using a facile solvothermal method (Fig. 7e) [141]. Revised Perdew-Burke-Ernzerhof (RPBE) density functional calculations were performed to prove that the glucose molecule could be adsorbed on the V_2O_5 nanozyme. Afterwards the first continuous monitoring enzyme-free online optical detection platform for glucose in rat brain using self-cascade V_2O_5 was developed via a microfluidic chip similar to the one mentioned above (Fig. 7f) [78]. The artificial cerebrospinal fluid (aCSF), V_2O_5, and TMB solution were mixed to initiate the cascaded colorimeter reaction. Then, the real-time light intensity profile of samples in capillary-based microfluidic system was recorded to monitor dynamic changes of glucose in the rat brain. In the self-cascade process, diffusion-limited kinetics need not be considered, demonstrating the advantages over highly specific natural enzymes. Based on microfluidics and self-cascade nanozyme, the glucose level could be detected successfully.

Since lots of nanozymes were proved to possess oxidase-like activity, it was possible to realize the cascade reaction between nanozymes. The cascade without enzyme participating could fully exhibit the advantages of nanozymes. The cost of microfluidic bioanalysis constructed by nanozyme would be greatly reduced. The ability of microfluidics to build reactions in sequence was even more convenient to construct biosensors by nanozymes solely. It was expected that more and more nanozymes with other oxidase-like activities would be used in bioanalysis.

3.3. *Improved selectivity by cascaded nanozymes in microfluidics*

Unlike the enzymes with exquisite structures, the lack of fine structures around active centers of nanozymes causes poor specificity. Therefore, many strategies have been considered to enhance the selectivity of nanozymes [34]. Except for combining the biorecognition elements such as coupling with enzyme, aptamer, and antibody, an efficient approach for engineering nanozymes with intrinsic specificity is to immobilize molecular imprinting sites onto nanozyme surface to serve as substrate binding pockets [144]. However, the polymer on the surface of nanozyme would lead to an undesirable decrease in activity. Thus, Liu et al. developed three kinds of light-responsive oxidase-like MOF-based nanozymes, with totally distinct structures. The different substrate specificity was obtained, and the unshielded active sites indicated unaffected oxidase-activity [145].

Chen et al. found that the bound M=O intermediate played an important role in the substrate selectivity of peroxidase-like catalysis of metal-N-C nanozymes [146]. Moreover, the bionic strategy of mimicking the natural active sites of enzymes is also an effective strategy to endow nanozymes with intrinsic specificity [147,148]. Inspired by HRP, Kim et al. designed a Fe—N_4 single site embedded graphene (Fe—N-rGO) with remarkable selectivity to H_2O_2 without any oxidizing activity [149].

The methods above could be applied to engineer nanozymes with intrinsic specificity for performing selective detection. Unexpectedly, cascaded microfluidics could be used to solve the vital problem in the nanozyme field. Recently, Zhou et al. proposed a strategy that enhanced the reaction selectivity by screening

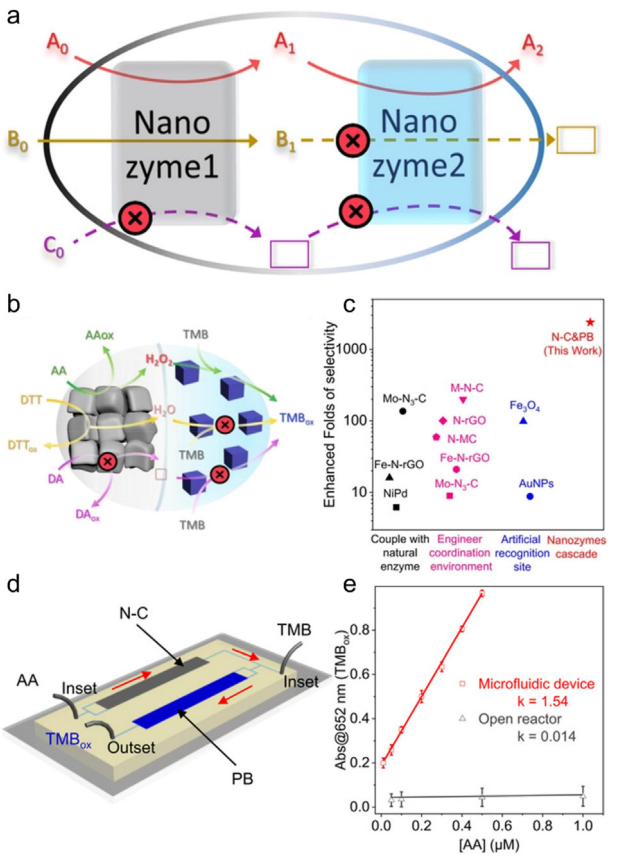

Fig. 8. Improved selectivity by cascaded nanozymes in microfluidics. (a) Schematic of operation principle of the nanozymes cascade. Two of three potential substrates can be catalyzed by Nanozyme1, while only one of them can be further screened out from the second cascaded reaction by Nanozyme2. (b) Schematic of cascade nanozyme reactions in a spatially confined reactor. (c) Comparison of the enhanced selectivity by nanozymes reported herein with those described in the literature (d) Schematic of cascade nanozyme reactions in a spatially confined microfluidics. (e) The calibration curves of oxidation and detection of AA in a microfluidic device compared to that in an open reactor. (a-e, reprinted with permission from Ref. [150]. Copyright (2021) John Wiley and Sons.).

substrates via cascade nanozymes. Under the ideal conditions, various substrates would be catalyzed by Nanozyme1 due to its poor selectivity. To overcome this challenge, Nanozyme2 was introduced to carry out the following process using product with higher priority by Nanozyme1 as the substrate (Fig. 8a) [150]. Based on this principle, a cascade reaction between oxidase-like N—C and peroxidase-like PB nanozyme with exceptionally high reaction selectivity for AA was achieved (Fig. 8b and c). By using the unique spatially confined microfluidic device, a more than 100-fold enhancement of the reaction efficiency was realized (Fig. 8d and e). In this study, the cascaded reaction in sequence provided by the microfluidic device endowed nanozymes with improved selectivity. The universal strategy provided by cascaded reactions in microfluidics made great contributions to selectivity of nanozyme systems. However, it was still a long way to go to fully tackle the selectivity problem.

The sensitive and selective detection could be achieved by cascaded reaction regardless of whether enzymes were involved or not due to the combination of microfluidics and nanozymes. Additionally, the cascaded system could be used to achieve the selectivity of nanozymes. Moreover, similar to the unexpected selectivity, more possibilities between microfluidics and cascaded nanozymes still need to be explored. Above all, the applications, analytical performances, and the role of microfluidics according to the nanozyme's type were listed in Table 1.

Table 1
Typical microfluidic bioanalyses based on nanozymes.

Nanozyme		Analyte	Mode	Detection range	LOD	Microfluidics	Ref.
Peroxidase-like nanozyme	$ZnFe_2O_4$–multiwalled carbon nanotubes	CEA	Colorimetric	0.005–30 ng/mL	2.6 pg/mL	Microfluidic paper-based analytical device (μPAD)	[151]
	Au@PdPt NPs	K562 cells	Electrochemical	1×10^2–2×10^7 cells/mL	31 cells/mL	Paper-based electrode	[152]
	INAzyme	Glucose	Colorimetric	0–250 μM	1.7 μM	Online microfluidic chip	[133]
	PdAu NPs	CEA	PEC	0.001–90 ng/mL	0.33 pg/mL	Paper-based electrode	[64]
	Pd/Fe_3O_4@C MNPs	CEA	Colorimetric	0.005–30 ng/mL	1.7 pg/mL	μPAD	[62]
		α-AFP		0.005–30 ng/mL	1.7 pg/mL		
	FA-pPdAu/GO	H_2O_2	Fluorometric	0.3–1 mM	0.1 nM	μPAD	[153]
	$ZnFe_2O_4$ MNPs	Bisphenol A	Colorimetric	10–1000 nM	6.18 nM	μPAD	[154]
	$CuFe_2O_4$/GQDs MNPs	Chlorpyrifos	Colorimetric	32–600 nM	10.7 nM	Microfluidic chip for samples mixing and analysis	[155]
	MIL-101	Glucose	Colorimetric	10.6–150 μM	2.5 μM	μPAD	[66]
	Fe_3O_4@GO	PSA	Electrochemical	61 fg/mL – 3.9 pg/mL	15 fg/mL	Microfluidic system for capturing analytes	[65]
		PMSA		9.8 fg/mL – 10 pg/mL	4.8 fg/mL		
	$Co_2(OH)_2CO_3$–CeO_2	CEA	Smartphone-based	0.002–75.0 ng/mL	0.51 pg/mL	μPAD	[156]
	Iron oxide	Targeted Gene	Electrochemical	0–1000 copies	50 copies-	Biochip for sample extraction, signal amplification and transduction	[67]
	$Mn_3(PO_4)_2$ H_2O	Glucose	Smartphone-based	0.1–20 mM	0.1 mM	μPAD	[130]
	CeO_2	miR-21	Electrochemical	1–1000 fM	0.434 fM	μPAD	[37]
			Colorimetric	10–1000 fM	7.382 fM		
	Cys-Au nanoclusters	Citrate	Colorimetric	1.0 μM–10 mM	0.4 μM	μPAD	[157]
	Co_3O_4–CeO_2 nanosheets	Glucose	Smartphone-based	0.005–1.5 mM	0.21 μM	μPAD	[158]
	Pt/Ni@NGT	Glucose	Colorimetric	43 pM–220 μM	1 pM	μPAD	[159]
	Au@PtNP/GO	H_2O_2	Electrochemical	1 μM–3 mM	1.62 μM	Microfluidic chip for sample handling and transduction	[160]
	$Co_{0.25}Zn_{0.75}Fe_2O_4$	CYFRA 21-1	Electrochemical	3.9–1000 fg/mL	0.19 fg/mL	Microfluidic chip for sample reaction, “Stop-Flow” controlling, and signal transduction	[161]
	Apt/g-C_3N_4 NS	STR	Fluorometric	0.05–30 ng/mL	23 pg/mL	μPAD for pH controlling, targets acquisition, “Stop-Flow” controlling.	[39]
		TOB		0.1–150 ng/mL	69 pg/mL		
		KANA		0.05–150 ng/mL	45 pg/mL		
	Au/Pt nanoclusters	*S. aureus*	Colorimetric	10^2–10^8 CFU/mL	80 CFU/mL	μPAD	[162]
	Ag/Pt nanoclusters	miR-21	Colorimetric	10–1000 pM	4.1 pM	μPAD	[163]
	MoO_x quantum dots	H_2O_2	Colorimetric	1–20 μM	175 nM	μPAD	[164]
	β-$Co(OH)_2$ CMK	Cytochrome *c*	Colorimetric	50 nM–1 mM	1 nM	μPAD	[165]
			Chemiluminescent	0.1 pM–1 nM	0.01 pM		
	NH_2-MIL-53(Fe)	Prostate specific antigen	Chemiluminescent	1–30 ng/mL	0.3 ng/mL	μPAD	[166]
			Fluorometric	0.5–30 ng/mL	0.2 ng/mL		
	CeO_2 @Au NPs	Pb^{2+}	Electrochemical	10 pM–5 μM	3.1 pM	Microfluidic chip for sample reaction, and signal transduction	[167]
	Fe_3O_4/C Dots	Parathion-methyl	Electrochemical	50 Pm–20 nM	11.6 pM	μPAD	[68]
	N-CDs	Total cholesterol	Colorimetric	2.5–7.5 mM	676 μM	Laminated 3D-μPAD	[129]
	NH_2-MIL-101(Fe)	*Salmonella*	Raspberry Pi based	1.5×10^1 to 1.5×10^7 CFU/mL	14 CFU/mL	Microfluidic chip for sample mixing and incubation	[168]
	Fe-UiO-66	Glucose	Electrochemical	2–24 mM	130 μM	Microfluidic channels for fast, accurate, and effective sampling	[131]
		Lactic acid		0.05–6 mM	3 nM		
		Cholesterol		0.1–10 mM	6 nM		
	MnO_2 NFs	*Salmonella*	Smartphone-based	4.4–4.4×10^6 CFU/mL	44 CFU/mL	Microfluidic chip for convergence–divergence spiral mixing	[41]
	COF@Pt	PCC-CTCs	Smartphone-based and electrochemical	2–10^5 cells/mL	1 cells/mL	Microfluidic chip for automatic cell sampling and detection	[46]
	MOF (Fe–Cu)	Choline	Colorimetric	20–200 μM	6 nM	μPAD	[169]
	PtNZHG	Glucose	Smartphone-based	0.01–10 mM	3.9 μM	Maintaining unidirectional liquid flow.	[170]
	Co-doped mesoporous ceria	H_2O_2	Smartphone-based	0.1–1.5 mM	5 μM	Multichannel μPAD	[132]
		Glucose		0.1–1.5 mM	7 μM		
		Galactose		0.1–4 mM	20 μM		
		Cholesterol		0.1–1.5 mM	8 μM		
		Choline		0.1–2 mM	7 μM		
		Acetylcholine		0.1–2 mM	11 μM		
	Au@Pt NCs	*Salmonella*	Smartphone-based	3.5×10^2–3.5×10^5 CFU/mL	350 CFU/mL	Finger-actuated micromixer	[171]
	Pt NPs	Glucose	Smartphone-based	0.01–5.0 mM	4 μM	Multichannel μPAD	[172]
		Uric acid		0.01–2.5 mM	3 μM		

(*continued on next page*)

Table 1 (*continued*)

Nanozyme		Analyte	Mode	Detection range	LOD	Microfluidics	Ref.
Oxidase-like nanozyme	CuO NPs	NSE	PEC Fluorometric	0.0001−150 ng/mL 0.001−150 ng/mL	28 fg/mL 250 fg/mL	Microfluidic chip for sample reaction, and signal transduction	[84]
	Nickel−iron PBA-incorporated MoSx	H_2S	Colorimetric	0.1−15 μM	33 nM	Online microfluidic chip	[86]
	Guanine-copper hybrid flower	Dopamine Catechol Hydroquinone	Smartphone-based	5−2.5 μg/mL 5−2.5 μg/mL 5−2.5 μg/mL	4.5 μg/mL 3 μg/mL 4.5 μg/mL	Multichannel μPAD	[83]
	ZIF-L-Co-Cys	Uric acid	Electrochemical	200 nM−50 μM	67 nM	Online microfluidic chip	[78]
Catalase-like nanozyme	Pt NPs	Target DNA	Distance	0−2 nM	20 pM	Microfluidic chip for signal amplification and transduction	[95]
	Au@Pt NPs	Cocaine	Distance	0−500 μM	0.06 μM	Microfluidic chip for signal amplification and transduction	[97]
	Pt NPs	CEA	Digital readout	0.1−1000 pM	0.1 pM	Microfluidic chip for signal amplification and transduction	[100]
	Pt NPs	CEA CYFRA 21-1 SCCA	Distance	0.05−250 ng/mL 0.05−375 ng/mL 0.05−250 ng/mL	down to ~50 pg/mL	Microfluidic chip for signal amplification and transduction	[104]
	Pt NPs	Aflatoxin B1	Distance	0.25−40 μM	1.77 nM	Microfluidic chip for signal amplification and transduction	[101]
	Pt NPs	PSA HCG	Distance	25−150 pM 10 pM−1 nM	12 pM 10 pM	Microfluidic chip for signal amplification and transduction	[102]
	Pt NPs	Cu^{2+} Pb^{2+} Hg^{2+}	Distance	1.5−258 nM 1.5−258 nM 2−200 nM	1 nM 1 nM 1.8 nM	Microfluidic chip for signal amplification and transduction	[107]
	Pt NPs	*E. coli* *S. aureus*	Distance	$1-10 \times 10^7$ CFU/mL $1-10 \times 10^7$ CFU/mL	1 CFU/mL 10 CFU/mL	Microfluidic chip for signal amplification and transduction	[38]
	Fe-MOF/PtNPs	*Salmonella typhimurium*	Temperature	$1.01 \times 10^2-1.01 \times 10^6$ CFU/mL	93 CFU/mL	Microfluidic chip for sample reaction, and signal transduction	[98]
	Pt NPs	HCG CEA	Colorimetric counting	10−250 mIU 1.28−173.75 ng/mL	2 mIU 1 ng/mL	Automatic washing and rapid analysis	[108]
SOD-like nanozyme	CTS-$Mn_3(PO_4)_2$	$O_2^{\bullet-}$	Electrochemical	57.9 nM−5 μM.	9.4 nM	Microfluidic chip for culturing cells and in situ electrical detection	[119]
	BC@DNA-$Mn_3(PO_4)_2$	$O_2^{\bullet-}$	Electrochemical	34.7 nM−7 μM	5.87 nM	Microfluidic chip for simultaneously culturing cells and in situ electrical detection	[122]

4. Conclusions and outlook

In this review, we summarized the recent advances in microfluidic bioanalysis based on nanozymes. The nanozymes with different enzyme-like activities and the cascade reactions involving nanozymes have made great progress in microfluidic bioanalysis. With the rapid development of the nanozyme field, it has attracted increasing interest and lots of excellent research has been performed [32]. Among them, LFA based test strips, V-chip, microfluidic covered electrode, and other microfluidics could fully utilize the advantages of nanozyme as significant labels to perform signal amplification. And various analytes (including heavy ion, biological macromolecule, virus, bacteria, *etc.*) could be successfully analyzed in sensitive, simple, cheap, and portable microfluidic devices. Meanwhile, the nanozymes possessed their own advantages as nanomaterials compared to their natural counterparts. Beyond artificial enzyme mimics, the unique optical, electrical, magnetic, and acoustic properties of nanozymes should also be explored to make more progress in microfluidics [85]. Moreover, different from the highly specific enzymes, the multienzyme-like activities of nanozymes could be regarded as a double-edged sword. On one hand, based on this, self-cascade biosensors could be constructed. On the other hand, the lack of specificity induced the poor selectivity for different analytes. Fortunately, the microfluidic technology and other strategies have been proposed to endow nanozymes with higher selectivity. For sensing strategies, the interaction (promote or inhibit) between analytes and nanozymes could be used to construct biosensors and pharmaceutical analysis [31,33,69].

For nanozymes, there are still some bottlenecks to be overcome for developing more smart biosensors in microfluidic bioanalysis. (1) More sensitive detection usually needs nanozymes with higher activity. In recent years, with the deepening of understanding toward nanozymes' mechanisms, nanozymes could be rationally designed to achieve higher activities [73,77]. In addition, it may be considered to construct a microfluidic chip composed of a nanozyme embedding polymer. (2) A higher specificity usually means more accurate detection, which should be carefully considered. More attention should be paid to the structure design of nanozymes to address this problem [173]. (3) The quality control and standardization of nanozymes should also be considered as soon as possible. Based on the standardized micro/nanofabrication technology, the commercial microfluidics could be easily fabricated. Considering further translational potentials to perform POC and bedside tests, the uniform nanozymes are strongly demanded. (4) More importantly, most efforts have been made to optimize and enhance sensing performance based on the existing principles rather than developing innovative strategies. Improving the system integration could synergize the advantages of microfluidics and nanozymes to realize more innovative applications. More types of nanozymes could be involved in microfluidic bioanalysis. For example, hydrolase-like nanozymes may be used in the analysis toward their substrates [174].

For microfluidic technology, the excellent reagents and analytes handling, sample processing and analysis, and easy-to-read capabilities have made microfluidics ideal candidates for sensing and detection. Though relying on these advantages, rapid and simple strips, sensitive and portable V-Chips, and real-time *in vivo* online monitoring have been advanced, the promise of microfluidics has not been fully explored yet. For example, ultrahigh-throughput screening using nanozymes could be realized. Moreover, single-cell metabolite analysis could be advanced using the unique sample isolating and manipulating properties [175,176]. Additionally, the nanozymes could be used in organ chips to refer to disease modeling, drug screening, and precision medicine [177,178]. In turn, existing microfluidics may be improved by the reaction catalyzed by nanozymes. For instance, fluids flow in microfluidic channels could be driven by the O_2 generated from catalase-like nanozymes. Nanozyme engineered polymers may provide microfluidic chips with enhanced performance, such as mechanical property and chemical stability.

Overall, the microfluidics will play an essential role in the POC diagnosis, such as in the global COVID-19 pandemic. Though considerable progress has been made in existing microfluidics, other components (enzyme and spectrometer in particular) are still needed under most complex circumstances. The all-nanozyme microfluidics are encouraged to be developed to make full use of their advantages. The realization of all-nanozyme microfluidics is required to develop multifunctional nanozymes with the ability of signal recognition and transduction. The surface engineering of nanozymes would be a good choice for signal recognition of nanozymes. Moreover, the self-reporting of nanozyme microfluidics in bioanalysis should be given enough attention, which will benefit their promotion among populations. For signal transduction, the distance droplets travelling is an excellent example. In addition, the therapeutic applications of microfluidics are now emerging. Therefore, based on the microfluidic bioanalysis, the theranostics could also be achieved by therapeutic nanozymes. Though there are still a few problems to be addressed, with more efforts of researchers of nanozymes and microfluidics, this field will embrace a promising future.

Declaration of competing interest

The authors declare that they have no known competing financial interests or personal relationships that could have appeared to influence the work reported in this paper.

Data availability

No data was used for the research described in the article.

Acknowledgements

This work was supported by grants from the National Natural Science Foundation of China (No. 21874129, 22174137, 21874067 and 21722503), the International Scientific Cooperation Project of Jilin Scientific and Technological Development Program (No. 20200801044GH), and the Key Research and Development Projects of Jilin Scientific and Technological Development Program (No. 202102041266YY).

References

[1] C. Zong, M. Xu, L.J. Xu, T. Wei, X. Ma, X.-S. Zheng, R. Hu, B. Ren, Surface-enhanced Raman spectroscopy for bioanalysis: reliability and challenges, Chem. Rev. 118 (2018) 4946.
[2] C. Shi, S. Goldberg, T. Lin, V. Dudkin, W. Widdison, L. Harris, S. Wilhelm, Y. Jmeian, D. Davis, K. O'Neil, N. Weng, W. Jian, LC/MS/MS bioanalysis of protein–drug conjugates—the importance of incorporating succinimide hydrolysis products, Anal. Chem. 90 (2018) 5314.
[3] A. Ahmad Dar, P.L. Sangwan, A. Kumar, Chromatography: an important tool for drug discovery, J. Separ. Sci. 43 (2020) 105.
[4] J. Wu, Z.Y. He, Q.S. Chen, J.M. Lin, Biochemical analysis on microfluidic chips, TrAC, Trends Anal. Chem. 80 (2016) 213.
[5] Y. Ai, R. Xie, J. Xiong, Q. Liang, Microfluidics for biosynthesizing: from droplets and vesicles to artificial cells, Small 16 (2020), e1903940.
[6] G.M. Whitesides, The origins and the future of microfluidics, Nature 442 (2006) 368.
[7] S. Battat, D.A. Weitz, G.M. Whitesides, An outlook on microfluidics: the promise and the challenge, Lab Chip 22 (2022) 530.
[8] T. Chen, S. Yin, J. Wu, Nanomaterials meet microfluidics: improved analytical methods and high-throughput synthetic approaches, TrAC, Trends Anal. Chem. 142 (2021), 116309.
[9] X.X. Qin, J.J. Liu, Z. Zhang, J.H. Li, L. Yuan, Z.Y. Zhang, L.X. Chen, Microfluidic paper-based chips in rapid detection: current status, challenges, and

perspectives, TrAC, Trends Anal. Chem. 143 (2021), 116371.
[10] V. Shirshahi, G. Liu, Enhancing the analytical performance of paper lateral flow assays: from chemistry to engineering, TrAC, Trends Anal. Chem. 136 (2021), 116200.
[11] M.A. Morales, J.M. Halpern, Guide to selecting a biorecognition element for biosensors, Bioconjugate Chem. 29 (2018) 3231.
[12] J.D. Newman, S.J. Setford, Enzymatic biosensors, Mol. Biotechnol. 32 (2006) 249.
[13] C.M. Cheng, A.W. Martinez, J. Gong, C.R. Mace, S.T. Phillips, E. Carrilho, K.A. Mirica, G.M. Whitesides, Paper-based ELISA, Angew. Chem., Int. Ed. Engl. 49 (2010) 4771.
[14] R.M. Lequin, Enzyme immunoassay (EIA)/Enzyme-Linked immunosorbent assay (ELISA), Clin. Chem. 51 (2005) 2415.
[15] D. Liu, F. Liu, Y. Huang, Y. Song, Z. Zhu, S.F. Zhou, C. Yang, Catalase-linked immunosorbent pressure assay for portable quantitative analysis, Analyst 144 (2019) 4188.
[16] J.R. Crowther, The ELISA Guidebook, Springer, 2009.
[17] S. Sakamoto, W. Putalun, S. Vimolmangkang, W. Phoolcharoen, Y. Shoyama, H. Tanaka, S. Morimoto, Enzyme-linked immunosorbent assay for the quantitative/qualitative analysis of plant secondary metabolites, J. Nat. Med. 72 (2018) 32.
[18] S.D. Gan, K.R. Patel, Enzyme immunoassay and enzyme-linked immunosorbent assay, J. Invest. Dermatol. 133 (2013) e12.
[19] L. Wu, G.H. Li, X. Xu, L. Zhu, R.M. Huang, X.Q. Chen, Application of nano-ELISA in food analysis: recent advances and challenges, TrAC, Trends Anal. Chem. 113 (2019) 140.
[20] P. Peng, C. Liu, Z.D. Li, Z.R. Xue, P. Mao, J. Hu, F. Xu, C.Y. Yao, M.L. You, Emerging ELISA derived technologies for in vitro diagnostics, TrAC, Trends Anal. Chem. 152 (2022), 116605.
[21] Q.Q. Wang, H. Wei, Z.Q. Zhang, E.K. Wang, S.J. Dong, Nanozyme: an emerging alternative to natural enzyme for biosensing and immunoassay, TrAC, Trends Anal. Chem. 105 (2018) 218.
[22] R. Breslow, Artificial enzymes, Science 218 (1982) 532.
[23] L. Gao, J. Zhuang, L. Nie, J. Zhang, Y. Zhang, N. Gu, T. Wang, J. Feng, D. Yang, S. Perrett, X. Yan, Intrinsic peroxidase-like activity of ferromagnetic nanoparticles, Nat. Nanotechnol. 2 (2007) 577.
[24] H. Wei, E. Wang, Nanomaterials with enzyme-like characteristics (nanozymes): next-generation artificial enzymes, Chem. Soc. Rev. 42 (2013) 6060.
[25] J. Wu, X. Wang, Q. Wang, Z. Lou, S. Li, Y. Zhu, L. Qin, H. Wei, Nanomaterials with enzyme-like characteristics (nanozymes): next-generation artificial enzymes (II), Chem. Soc. Rev. 48 (2019) 1004.
[26] Y. Huang, J. Ren, X. Qu, Nanozymes: classification, catalytic mechanisms, activity regulation, and applications, Chem. Rev. 119 (2019) 4357.
[27] H. Wei, L.Z. Gao, K.L. Fan, J.W. Liu, J.Y. He, X.G. Qu, S.J. Dong, E.K. Wang, X.Y. Yan, Nanozymes, A clear definition with fuzzy edges, Nano Today 40 (2021), 101269.
[28] Z. Tu, Y. Zhong, H. Hu, D. Shao, R. Haag, M. Schirner, J. Lee, B. Sullenger, K.W. Leong, Design of therapeutic biomaterials to control inflammation, Nat. Rev. Mater. 7 (2022) 557.
[29] M. Soh, D.W. Kang, H.G. Jeong, D. Kim, D.Y. Kim, W. Yang, C. Song, S. Baik, I.Y. Choi, S.K. Ki, H.J. Kwon, T. Kim, C.K. Kim, S.H. Lee, T. Hyeon, Ceria-Zirconia nanoparticles as an enhanced multi-antioxidant for sepsis treatment, Angew. Chem., Int. Ed. Engl. 56 (2017), 11399.
[30] K. Fan, J. Xi, L. Fan, P. Wang, C. Zhu, Y. Tang, X. Xu, M. Liang, B. Jiang, X. Yan, L. Gao, In vivo guiding nitrogen-doped carbon nanozyme for tumor catalytic therapy, Nat. Commun. 9 (2018) 1440.
[31] Y. Xu, J. Xue, Q. Zhou, Y. Zheng, X. Chen, S. Liu, Y. Shen, Y. Zhang, The Fe-N-C nanozyme with both accelerated and inhibited biocatalytic activities capable of accessing drug-drug interactions, Angew. Chem., Int. Ed. Engl. 59 (2020), 14498.
[32] S. Li, Y. Zhang, Q. Wang, A. Lin, H. Wei, Nanozyme-enabled analytical chemistry, Anal. Chem. 94 (2022) 312.
[33] Q. Wang, S. Liu, Z. Tang, Recent progress in the design of analytical methods based on nanozymes, J. Mater. Chem. B 9 (2021) 8174.
[34] X. Li, H.J. Zhu, P. Liu, M.Z. Wang, J.M. Pan, F.X. Qiu, L. Ni, X.H. Niu, Realizing selective detection with nanozymes: strategies and trends, TrAC, Trends Anal. Chem. 143 (2021), 116379.
[35] Y. Shi, Z. Liu, R. Liu, R. Wu, J.J. Zhang, DNA-encoded MXene-Pt nanozyme for enhanced colorimetric sensing of mercury ions, Chem. Eng. J. 442 (2022), 136072.
[36] S.G. Jeong, D.H. Kim, J. Kim, J.H. Kim, S. Song, C.S. Lee, Programmable microfluidic flow for automatic multistep digital assay in a single-sheet 3-dimensional paper-based microfluidic device, Chem. Eng. J. 411 (2021), 128429.
[37] X. Sun, H. Wang, Y. Jian, F. Lan, L. Zhang, H. Liu, S. Ge, J. Yu, Ultrasensitive microfluidic paper-based electrochemical/visual biosensor based on spherical-like cerium dioxide catalyst for miR-21 detection, Biosens. Bioelectron. 105 (2018) 218.
[38] T. Huang, J.J. Yang, W.Q. Zhou, X.L. Liu, Y.C. Pan, Y.J. Song, Rapid identification of urinary tract infections based on ultrasensitive bacteria detection using volumetric bar-chart chip, Sens. Actuators, B 298 (2019), 126885.
[39] L. Wang, F. Zhu, Y. Zhu, S. Xie, M. Chen, Y. Xiong, Q. Liu, H. Yang, X. Chen, Intelligent platform for simultaneous detection of multiple aminoglycosides based on a ratiometric paper-based device with digital fluorescence detector readout, ACS Sens. 4 (2019) 3283.
[40] Q. Xu, Y. Pan, X. Liu, Y. Gao, X. Luan, F. Zeng, D. Zhou, W. Long, Y. Wang, Y. Song, Hypoxia-responsive platinum supernanoparticles for urinary microfluidic monitoring of tumors, Angew. Chem., Int. Ed. Engl. 61 (2022), e202114239.
[41] L. Xue, N. Jin, R. Guo, S. Wang, W. Qi, Y. Liu, Y. Li, J. Lin, Microfluidic colorimetric biosensors based on MnO_2 nanozymes and convergence-divergence spiral micromixers for rapid and sensitive detection of *Salmonella*, ACS Sens. 6 (2021) 2883.
[42] X. Shen, Z. Wang, X. Gao, Y. Zhao, Density functional theory-based method to predict the activities of nanomaterials as peroxidase mimics, ACS Catal. 10 (2020), 12657.
[43] H. Dong, W. Du, J. Dong, R. Che, F. Kong, W. Cheng, M. Ma, N. Gu, Y. Zhang, Depletable peroxidase-like activity of Fe3O4 nanozymes accompanied with separate migration of electrons and iron ions, Nat. Commun. 13 (2022) 5365.
[44] W. Zhang, S. Hu, J.J. Yin, W. He, W. Lu, M. Ma, N. Gu, Y. Zhang, Prussian blue nanoparticles as multienzyme mimetics and reactive oxygen species scavengers, J. Am. Chem. Soc. 138 (2016) 5860.
[45] Z. Xi, K. Wei, Q. Wang, M.J. Kim, S. Sun, V. Fung, X. Xia, Nickel-platinum nanoparticles as peroxidase mimics with a record high catalytic efficiency, J. Am. Chem. Soc. 143 (2021) 2660.
[46] X. Liu, F. Wang, Y. Meng, L. Zhao, W. Shi, X. Wang, Z. He, J. Chao, C. Li, Electrochemical/visual microfluidic detection with a covalent organic framework supported platinum nanozyme-based device for early diagnosis of pheochromocytoma, Biosens. Bioelectron. 207 (2022), 114208.
[47] Z. Farka, V. Cunderlova, V. Horackova, M. Pastucha, Z. Mikusova, A. Hlavacek, P. Skladal, Prussian blue nanoparticles as a catalytic label in a sandwich nanozyme-linked immunosorbent assay, Anal. Chem. 90 (2018) 2348.
[48] M. Yan, G. Chen, Y. She, J. Ma, S. Hong, Y. Shao, A.M. Abd El-Aty, M. Wang, S. Wang, J. Wang, Sensitive and simple competitive biomimetic nanozyme-linked immunosorbent assay for colorimetric and surface-enhanced Raman scattering sensing of triazophos, J. Agric. Food Chem. 67 (2019) 9658.
[49] M. Broto, M.M. Kaminski, C. Adrianus, N. Kim, R. Greensmith, S. Dissanayake-Perera, A.J. Schubert, X. Tan, H. Kim, A.S. Dighe, J.J. Collins, M.M. Stevens, Nanozyme-catalysed CRISPR assay for preamplification-free detection of non-coding RNAs, Nat. Nanotechnol. 17 (2022) 1120.
[50] S.E. Lohse, C.J. Murphy, Applications of colloidal inorganic nanoparticles: from medicine to energy, J. Am. Chem. Soc. 134 (2012), 15607.
[51] D. Duan, K. Fan, D. Zhang, S. Tan, M. Liang, Y. Liu, J. Zhang, P. Zhang, W. Liu, X. Qiu, G.P. Kobinger, G.F. Gao, X. Yan, Nanozyme-strip for rapid local diagnosis of Ebola, Biosens. Bioelectron. 74 (2015) 134.
[52] N. Cheng, Y. Song, M.M.A. Zeinhom, Y.C. Chang, L. Sheng, H. Li, D. Du, L. Li, M.J. Zhu, Y. Luo, W. Xu, Y. Lin, Nanozyme-mediated dual immunoassay integrated with smartphone for use in simultaneous detection of pathogens, ACS Appl. Mater. Interfaces 9 (2017), 40671.
[53] J. Han, L. Zhang, L. Hu, K. Xing, X. Lu, Y. Huang, J. Zhang, W. Lai, T. Chen, Nanozyme-based lateral flow assay for the sensitive detection of Escherichia coli O157:H7 in milk, J. Dairy Sci. 101 (2018) 5770.
[54] Y. Zhao, M. Yang, Q. Fu, H. Ouyang, W. Wen, Y. Song, C. Zhu, Y. Lin, D. Du, A nanozyme- and ambient light-based smartphone platform for simultaneous detection of dual biomarkers from exposure to organophosphorus pesticides, Anal. Chem. 90 (2018) 7391.
[55] C.N. Loynachan, M.R. Thomas, E.R. Gray, D.A. Richards, J. Kim, B.S. Miller, J.C. Brookes, S. Agarwal, V. Chudasama, R.A. McKendry, M.M. Stevens, Platinum nanocatalyst amplification: redefining the gold standard for lateral flow immunoassays with ultrabroad dynamic range, ACS Nano 12 (2018) 279.
[56] B. Gates, Responding to covid-19 - a once-in-a-century pandemic? N. Engl. J. Med. 382 (2020) 1677.
[57] T. Ji, Z. Liu, G. Wang, X. Guo, S. Akbar Khan, C. Lai, H. Chen, S. Huang, S. Xia, B. Chen, H. Jia, Y. Chen, Q. Zhou, Detection of COVID-19: a review of the current literature and future perspectives, Biosens. Bioelectron. 166 (2020), 112455.
[58] D. Liu, C. Ju, C. Han, R. Shi, X. Chen, D. Duan, J. Yan, X. Yan, Nanozyme chemiluminescence paper test for rapid and sensitive detection of SARS-CoV-2 antigen, Biosens. Bioelectron. 173 (2020), 112817.
[59] H. Nikaido, Multidrug resistance in bacteria, Annu. Rev. Biochem. 78 (2009) 119.
[60] H. Sun, S. Cai, C. Wang, Y. Chen, R. Yang, Recent progress of nanozymes in the detection of pathogenic microorganisms, Chembiochem 21 (2020) 2572.
[61] N. Sanvicens, C. Pastells, N. Pascual, M.P. Marco, Nanoparticle-based biosensors for detection of pathogenic bacteria, TrAC, Trends Anal. Chem. 28 (2009) 1243.
[62] L. Liang, S. Ge, L. Li, F. Liu, J. Yu, Microfluidic paper-based multiplex colorimetric immunodevice based on the catalytic effect of Pd/Fe_3O_4@C peroxidase mimetics on multiple chromogenic reactions, Anal. Chim. Acta 862 (2015) 70.
[63] L. Li, Y. Zhang, L. Zhang, S. Ge, H. Liu, N. Ren, M. Yan, J. Yu, Paper-based device for colorimetric and photoelectrochemical quantification of the flux of H_2O_2 releasing from MCF-7 cancer cells, Anal. Chem. 88 (2016) 5369.
[64] F. Lan, G. Sun, L. Liang, S. Ge, M. Yan, J. Yu, Microfluidic paper-based analytical device for photoelectrochemical immunoassay with multiplex signal amplification using multibranched hybridization chain reaction and PdAu enzyme mimetics, Biosens. Bioelectron. 79 (2016) 416.
[65] M. Sharafeldin, G.W. Bishop, S. Bhakta, A. El-Sawy, S.L. Suib, J.F. Rusling, Fe_3O_4 nanoparticles on graphene oxide sheets for isolation and ultrasensitive

amperometric detection of cancer biomarker proteins, Biosens. Bioelectron. 91 (2017) 359.
[66] I. Ortiz-Gomez, A. Salinas-Castillo, A.G. Garcia, J.A. Alvarez-Bermejo, I. de Orbe-Paya, A. Rodriguez-Dieguez, L.F. Capitan-Vallvey, Microfluidic paper-based device for colorimetric determination of glucose based on a metal-organic framework acting as peroxidase mimetic, Microchim. Acta 185 (2017) 47.
[67] K.M. Koo, S. Dey, M. Trau, A sample-to-targeted gene analysis biochip for nanofluidic manipulation of solid-phase circulating tumor nucleic acid amplification in liquid biopsies, ACS Sens. 3 (2018) 2597.
[68] S. Li, C. Pang, X. Ma, Y. Zhang, Z. Xu, J. Li, M. Zhang, M. Wang, Microfluidic paper-based chip for parathion-methyl detection based on a double catalytic amplification strategy, Microchim. Acta 188 (2021) 438.
[69] Y. Chang, S. Gao, M. Liu, J. Liu, Designing signal-on sensors by regulating nanozyme activity, Anal. Methods 12 (2020) 4708.
[70] X. Shen, W. Liu, X. Gao, Z. Lu, X. Wu, X. Gao, Mechanisms of oxidase and superoxide dismutation-like activities of gold, silver, platinum, and palladium, and their alloys: a general way to the activation of molecular oxygen, J. Am. Chem. Soc. 137 (2015), 15882.
[71] M. Li, J. Chen, W. Wu, Y. Fang, S. Dong, Oxidase-like MOF-818 nanozyme with high specificity for catalysis of catechol oxidation, J. Am. Chem. Soc. 142 (2020), 15569.
[72] Y. Chong, Q. Liu, C.C. Ge, Advances in oxidase-mimicking nanozymes: classification, activity regulation and biomedical applications, Nano Today 37 (2021), 101076.
[73] Z.Z. Wang, X.M. Shen, X.F. Gao, Density functional theory mechanistic insight into the peroxidase- and oxidase-like activities of nanoceria, J. Phys. Chem. C 125 (2021), 23098.
[74] X. Chen, C. Zhu, Y. Xu, K. Wang, X. Cao, Y. Shen, S. Liu, Y. Zhang, Quantitative evaluation of O_2 activation half-reaction for Fe—N—C in oxidase-like activity enhancement, Catal. Sci. Technol. 11 (2021) 7255.
[75] F. He, L. Mi, Y. Shen, T. Mori, S. Liu, Y. Zhang, Fe-N-C artificial enzyme: activation of oxygen for dehydrogenation and monoxygenation of organic substrates under mild condition and cancer therapeutic application, ACS Appl. Mater. Interfaces 10 (2018), 35327.
[76] R. Ragg, F. Natalio, M.N. Tahir, H. Janssen, A. Kashyap, D. Strand, S. Strand, W. Tremel, Molybdenum trioxide nanoparticles with intrinsic sulfite oxidase activity, ACS Nano 8 (2014) 5182.
[77] J. Chen, Q. Ma, M. Li, D. Chao, L. Huang, W. Wu, Y. Fang, S. Dong, Glucose-oxidase like catalytic mechanism of noble metal nanozymes, Nat. Commun. 12 (2021) 3375.
[78] G. Ren, F. Dong, Z. Zhao, K. Li, Y. Lin, Structure defect tuning of metal-organic frameworks as a nanozyme regulatory strategy for selective online electrochemical analysis of uric acid, ACS Appl. Mater. Interfaces 13 (2021), 52987.
[79] A.B. Ganganboina, R.A. Doong, The biomimic oxidase activity of layered V_2O_5 nanozyme for rapid and sensitive nanomolar detection of glutathione, Sens. Actuators, B 273 (2018) 1179.
[80] Y. Wu, L. Jiao, X. Luo, W. Xu, X. Wei, H. Wang, H. Yan, W. Gu, B.Z. Xu, D. Du, Y. Lin, C. Zhu, Oxidase-like Fe-N-C single-atom nanozymes for the detection of acetylcholinesterase activity, Small 15 (2019), e1903108.
[81] Q.M. Chen, S.Q. Li, Y. Liu, X.D. Zhang, Y. Tang, H.X. Chai, Y.M. Huang, Size-controllable Fe-N/C single-atom nanozyme with exceptional oxidase-like activity for sensitive detection of alkaline phosphatase, Sens. Actuators, B 305 (2020), 127511.
[82] Q. Wang, X. Wang, H. Wei, Spinel-oxide-based laccase mimics for the identification and differentiation of phenolic pollutants, Anal. Chem. 94 (2022), 10198.
[83] T.D. Tran, P.T. Nguyen, T.N. Le, M.I. Kim, DNA-copper hybrid nanoflowers as efficient laccase mimics for colorimetric detection of phenolic compounds in paper microfluidic devices, Biosens, Bioelectron 182 (2021), 113187.
[84] T. Wu, S. Yu, L. Dai, J. Feng, X. Ren, H. Ma, X. Wang, Q. Wei, H. Ju, CuO nanozymes as multifunctional signal labels for efficiently quenching the photocurrent of ZnO/Au/$AgSbS_2$ hybrids and initiating a strong fluorescent signal in a dual-mode microfluidic sensing platform, ACS Sens. 7 (2022) 1732.
[85] T.Y. Chen, S. Yin, J. Wu, Nanomaterials meet microfluidics: improved analytical methods and high-throughput synthetic approaches, TrAC, Trends Anal. Chem. 142 (2021), 116309.
[86] C. Wang, G. Ren, B. Yuan, W. Zhang, M. Lu, J. Liu, K. Li, Y. Lin, Enhancing enzyme-like activities of prussian blue analog nanocages by molybdenum doping: toward cytoprotecting and online optical hydrogen sulfide monitoring, Anal. Chem. 92 (2020) 7822.
[87] D. Richter, Decomposition of hydrogen peroxide by catalase, Nature 129 (1932) 870.
[88] R. Lemberg, E.C. Foulkes, Reaction between catalase and hydrogen peroxide, Nature 161 (1948) 131.
[89] M. Alfonso-Prieto, X. Biarnes, P. Vidossich, C. Rovira, The molecular mechanism of the catalase reaction, J. Am. Chem. Soc. 131 (2009), 11751.
[90] A. Lin, Q. Liu, Y. Zhang, Q. Wang, S. Li, B. Zhu, L. Miao, Y. Du, S. Zhao, H. Wei, A dopamine-enabled universal assay for catalase and catalase-like nanozymes, Anal. Chem. 94 (2022), 10636.
[91] J. Li, W. Liu, X. Wu, X. Gao, Mechanism of pH-switchable peroxidase and catalase-like activities of gold, silver, platinum and palladium, Biomaterials 48 (2015) 37.
[92] C. Wang, Y. Li, W. Yang, L. Zhou, S. Wei, Nanozyme with robust catalase activity by multiple mechanisms and its application for hypoxic tumor treatment, Adv. Healthcare Mater. 10 (2021), e2100601.
[93] Y. Zhang, Y. Jin, H. Cui, X. Yan, K. Fan, Nanozyme-based catalytic theranostics, RSC Adv. 10 (2019) 10.
[94] H.J. Kwon, M.Y. Cha, D. Kim, D.K. Kim, M. Soh, K. Shin, T. Hyeon, I. Mook-Jung, Mitochondria-targeting ceria nanoparticles as antioxidants for alzheimer's disease, ACS Nano 10 (2016) 2860.
[95] Y. Song, Y. Wang, L. Qin, A multistage volumetric bar chart chip for visualized quantification of DNA, J. Am. Chem. Soc. 135 (2013), 16785.
[96] Y. Song, Y. Zhang, P.E. Bernard, J.M. Reuben, N.T. Ueno, R.B. Arlinghaus, Y. Zu, L. Qin, Multiplexed volumetric bar-chart chip for point-of-care diagnostics, Nat. Commun. 3 (2012) 1283.
[97] Z. Zhu, Z. Guan, S. Jia, Z. Lei, S. Lin, H. Zhang, Y. Ma, Z.Q. Tian, C.J. Yang, Au@Pt nanoparticle encapsulated target-responsive hydrogel with volumetric bar-chart chip readout for quantitative point-of-care testing, Angew. Chem., Int. Ed. Engl. 53 (2014), 12503.
[98] R. Guo, L. Xue, G. Cai, W. Qi, Y. Liu, J. Lin, Fe-MIL-88NH_2 metal—organic framework nanocubes decorated with Pt nanoparticles for the detection of *Salmonella*, ACS Appl. Nano Mater. 4 (2021) 5115.
[99] Y. Song, X. Xia, X. Wu, P. Wang, L. Qin, Integration of platinum nanoparticles with a volumetric bar-chart chip for biomarker assays, Angew. Chem., Int. Ed. Engl. 53 (2014), 12451.
[100] Y. Li, J. Xuan, Y. Song, P. Wang, L. Qin, A microfluidic platform with digital readout and ultra-low detection limit for quantitative point-of-care diagnostics, Lab Chip 15 (2015) 3300.
[101] Y. Ma, Y. Mao, D. Huang, Z. He, J. Yan, T. Tian, Y. Shi, Y. Song, X. Li, Z. Zhu, L. Zhou, C.J. Yang, Portable visual quantitative detection of aflatoxin B1 using a target-responsive hydrogel and a distance-readout microfluidic chip, Lab Chip 16 (2016) 3097.
[102] Y. Xie, X. Wei, Q. Yang, Z. Guan, D. Liu, X. Liu, L. Zhou, Z. Zhu, Z. Lin, C. Yang, A Shake&Read distance-based microfluidic chip as a portable quantitative readout device for highly sensitive point-of-care testing, Chem. Commun. 52 (2016), 13377.
[103] Y. Song, Y. Wang, W. Qi, Y. Li, J. Xuan, P. Wang, L. Qin, Integrative volumetric bar-chart chip for rapid and quantitative point-of-care detection of myocardial infarction biomarkers, Lab Chip 16 (2016) 2955.
[104] Y. Li, J. Xuan, Y. Song, W. Qi, B. He, P. Wang, L. Qin, Nanoporous glass integrated in volumetric bar-chart chip for point-of-care diagnostics of non-small cell lung cancer, ACS Nano 10 (2016) 1640.
[105] Y. Wang, G. Zhu, W. Qi, Y. Li, Y. Song, A versatile quantitation platform based on platinum nanoparticles incorporated volumetric bar-chart chip for highly sensitive assays, Biosens. Bioelectron. 85 (2016) 777.
[106] D. Liu, X. Li, J. Zhou, S. Liu, T. Tian, Y. Song, Z. Zhu, L. Zhou, T. Ji, C. Yang, A fully integrated distance readout ELISA-Chip for point-of-care testing with sample-in-answer-out capability, Biosens. Bioelectron. 96 (2017) 332.
[107] X. Liu, Y. Wang, Y. Song, Visually multiplexed quantitation of heavy metal ions in water using volumetric bar-chart chip, Biosens. Bioelectron. 117 (2018) 644.
[108] J. Yang, X.L. Liu, Y.C. Pan, J.J. Yang, B.S. He, Y.Z. Fu, Y.J. Song, A self-powered microfluidic chip integrated with fluorescent microscopic counting for biomarkers assay, Sens. Actuators, B 291 (2019) 192.
[109] L. Sun, Q. Zhao, X. Liu, Y. Pan, Y. Gao, J. Yang, Y. Wang, Y. Song, Enzyme-mimicking accelerated signal enhancement for visually multiplexed quantitation of telomerase activity, Chem. Commun. 56 (2020) 6969.
[110] S. Lee, D. Kwon, C. Yim, S. Jeon, Facile detection of Troponin I using dendritic platinum nanoparticles and capillary tube indicators, Anal. Chem. 87 (2015) 5004.
[111] Z. Zhu, Z. Guan, D. Liu, S. Jia, J. Li, Z. Lei, S. Lin, T. Ji, Z. Tian, C.J. Yang, Translating molecular recognition into a pressure signal to enable rapid, sensitive, and portable biomedical analysis, Angew. Chem., Int. Ed. Engl. 54 (2015), 10448.
[112] Z. Yu, Y. Tang, G. Cai, R. Ren, D. Tang, Paper electrode-based flexible pressure sensor for point-of-care immunoassay with digital multimeter, Anal. Chem. 91 (2019) 1222.
[113] Y. Zhang, Q. Liu, C.B. Ma, Q. Wang, M. Yang, Y. Du, Point-of-care assay for drunken driving with Pd@Pt core-shell nanoparticles-decorated ploy(vinyl alcohol) aerogel assisted by portable pressure meter, Theranostics 10 (2020) 5064.
[114] Y. Sheng, I.A. Abreu, D.E. Cabelli, M.J. Maroney, A.F. Miller, M. Teixeira, J.S. Valentine, Superoxide dismutases and superoxide reductases, Chem. Rev. 114 (2014) 3854.
[115] Z. Wang, J. Wu, J.J. Zheng, X. Shen, L. Yan, H. Wei, X. Gao, Y. Zhao, Accelerated discovery of superoxide-dismutase nanozymes via high-throughput computational screening, Nat. Commun. 12 (2021) 6866.
[116] H. Zhao, R. Zhang, X. Yan, K. Fan, Superoxide dismutase nanozymes: an emerging star for anti-oxidation, J. Mater. Chem. B 9 (2021) 6939.
[117] X.Q. Ma, W.H. Hu, C.X. Guo, L. Yu, L.X. Gao, J.L. Xie, C.M. Li, DNA-templated biomimetic enzyme sheets on carbon nanotubes to sensitively in situ detect superoxide anions released from cells, Adv. Funct. Mater. 24 (2014) 5897.
[118] X. Cai, L. Shi, W. Sun, H. Zhao, H. Li, H. He, M. Lan, A facile way to fabricate manganese phosphate self-assembled carbon networks as efficient electrochemical catalysts for real-time monitoring of superoxide anions released from HepG2 cells, Biosens, Bioelectron 102 (2018) 171.
[119] Y. Wang, D. Wang, L.H. Sun, P. Xue, M.Q. Wang, Z. Lu, F. Wang, Q. Xia, M.W. Xu, S.J. Bao, Constructing high effective nano-$Mn_3(PO_4)_2$-chitosan in

situ electrochemical detection interface for superoxide anions released from living cell, Biosens. Bioelectron. 133 (2019) 133.
[120] X. Wang, M. Han, J. Bao, W. Tu, Z. Dai, A superoxide anion biosensor based on direct electron transfer of superoxide dismutase on sodium alginate sol-gel film and its application to monitoring of living cells, Anal. Chim. Acta 717 (2012) 61.
[121] S.Y. Lu, Y. Lu, M. Jin, S.J. Bao, W.Y. Li, L. Yu, Design and fabrication of highly sensitive and stable biochip for glucose biosensing, Appl. Surf. Sci. 422 (2017) 900.
[122] Y. Wang, D. Wang, L.H. Sun, L.C. Zhang, Z.S. Lu, P. Xue, F. Wang, Q.Y. Xia, S.J. Bao, BC@DNA-$Mn_3(PO_4)_2$ nanozyme for real-time detection of superoxide from living cells, Anal. Chem. 92 (2020), 15927.
[123] J.M. Sperl, V. Sieber, Multienzyme cascade reactions-status and recent advances, ACS Catal. 8 (2018) 2385.
[124] L.J. Reed, Multienzyme complexes, Acc. Chem. Res. 7 (1974) 40.
[125] Q. Wu, Z. He, X. Wang, Q. Zhang, Q. Wei, S. Ma, C. Ma, J. Li, Q. Wang, Cascade enzymes within self-assembled hybrid nanogel mimicked neutrophil lysosomes for singlet oxygen elevated cancer therapy, Nat. Commun. 10 (2019) 240.
[126] S. Fornera, P. Kuhn, D. Lombardi, A.D. Schluter, P.S. Dittrich, P. Walde, Sequential immobilization of enzymes in microfluidic channels for cascade reactions, ChemPlusChem 77 (2012) 98.
[127] X.L. Cai, L. Jiao, H.Y. Yan, Y. Wu, W.L. Gu, D. Du, Y.H. Lin, C.Z. Zhu, Nanozyme-involved biomimetic cascade catalysis for biomedical applications, Mater. Today 44 (2021) 211.
[128] H. Wei, E. Wang, Fe_3O_4 magnetic nanoparticles as peroxidase mimetics and their applications in H_2O_2 and glucose detection, Anal. Chem. 80 (2008) 2250.
[129] N. Kitchawengkul, A. Prakobkij, W. Anutrasakda, N. Yodsin, S. Jungsuttiwong, S. Chunta, M. Amatatongchai, P. Jarujamrus, Mimicking peroxidase-like activity of nitrogen-doped carbon dots (N-CDs) coupled with a laminated three-dimensional microfluidic paper-based analytical device (laminated 3D-μPAD) for smart sensing of total cholesterol from whole blood, Anal. Chem. 93 (2021) 6989.
[130] W. Li, S. Lu, S. Bao, Z. Shi, Z. Lu, C. Li, L. Yu, Efficient in situ growth of enzyme-inorganic hybrids on paper strips for the visual detection of glucose, Biosens. Bioelectron. 99 (2018) 603.
[131] H. Wu, T. Li, Y. Bao, X. Zhang, C. Wang, C. Wei, Z. Xu, W. Tong, D. Chen, X. Huang, MOF-enzyme hybrid nanosystem decorated 3D hollow fiber membranes for in-situ blood separation and biosensing array, Biosens. Bioelectron. 190 (2021), 113413.
[132] P.T. Nguyen, J. Lee, A. Cho, M.S. Kim, D. Choi, J.W. Han, M.I. Kim, J. Lee, Rational development of Co-doped mesoporous ceria with high peroxidase-mimicking activity at neutral pH for paper-based colorimetric detection of multiple biomarkers, Adv. Funct. Mater. 32 (2022), 2112428.
[133] H. Cheng, L. Zhang, J. He, W. Guo, Z. Zhou, X. Zhang, S. Nie, H. Wei, Integrated nanozymes with nanoscale proximity for in vivo neurochemical monitoring in living brains, Anal. Chem. 88 (2016) 5489.
[134] X. Liu, X. Mei, J. Yang, Y. Li, Hydrogel-involved colorimetric platforms based on layered double oxide nanozymes for point-of-care detection of liver-related biomarkers, ACS Appl. Mater. Interfaces 14 (2022) 6985.
[135] Y. Liu, X. Wei, J. Chen, Y.L. Yu, J.H. Wang, H. Qiu, Acetylcholinesterase activity monitoring and natural anti-neurological disease drug screening via rational design of deep eutectic solvents and CeO_2-$Co(OH)_2$ nanosheets, Anal. Chem. 94 (2022) 5970.
[136] X. Jiang, X. Wang, A. Lin, H. Wei, In situ exsolution of noble-metal nanoparticles on perovskites as enhanced peroxidase mimics for bioanalysis, Anal. Chem. 93 (2021) 5954.
[137] P.B. O'Mara, P. Wilde, T.M. Benedetti, C. Andronescu, S. Cheong, J.J. Gooding, R.D. Tilley, W. Schuhmann, Cascade reactions in nanozymes: spatially separated active sites inside Ag-Core-Porous-Cu-shell nanoparticles for multistep carbon dioxide reduction to higher organic molecules, J. Am. Chem. Soc. 141 (2019), 14093.
[138] Y. Liu, Y. Cheng, H. Zhang, M. Zhou, Y. Yu, S. Lin, B. Jiang, X. Zhao, L. Miao, C.W. Wei, Q. Liu, Y.W. Lin, Y. Du, C.J. Butch, H. Wei, Integrated cascade nanozyme catalyzes in vivo ROS scavenging for anti-inflammatory therapy, Sci. Adv. 6 (2020), eabb2695.
[139] J. Li, Z. Gao, H. Ye, S. Wan, M. Pierce, D. Tang, X. Xia, A non-enzyme cascade amplification strategy for colorimetric assay of disease biomarkers, Chem. Commun. 53 (2017) 9055.
[140] P. Zhang, D. Sun, A. Cho, S. Weon, S. Lee, J. Lee, J.W. Han, D.P. Kim, W. Choi, Modified carbon nitride nanozyme as bifunctional glucose oxidase-peroxidase for metal-free bioinspired cascade photocatalysis, Nat. Commun. 10 (2019) 940.
[141] Y. Ding, G. Ren, G. Wang, M. Lu, J. Liu, K. Li, Y. Lin, V_2O_5 nanobelts mimick tandem enzymes to achieve nonenzymatic online monitoring of glucose in living rat brain, Anal. Chem. 92 (2020) 4583.
[142] X. Meng, D. Li, L. Chen, H. He, Q. Wang, C. Hong, J. He, X. Gao, Y. Yang, B. Jiang, G. Nie, X. Yan, L. Gao, K. Fan, High-performance self-cascade pyrite nanozymes for apoptosis-ferroptosis synergistic tumor therapy, ACS Nano 15 (2021) 5735.
[143] X. Zhang, S. Zhang, Z. Yang, Z. Wang, X. Tian, R. Zhou, Self-cascade MoS_2 nanozymes for efficient intracellular antioxidation and hepatic fibrosis therapy, Nanoscale 13 (2021), 12613.
[144] Z. Zhang, X. Zhang, B. Liu, J. Liu, Molecular imprinting on inorganic nanozymes for hundred-fold enzyme specificity, J. Am. Chem. Soc. 139 (2017) 5412.
[145] Y. Liu, X. Wang, Q. Wang, Y. Zhang, Q. Liu, S. Liu, S. Li, Y. Du, H. Wei, Structurally engineered light-responsive nanozymes for enhanced substrate specificity, Anal. Chem. 93 (2021), 15150.
[146] X. Chen, L. Zhao, K. Wu, H. Yang, Q. Zhou, Y. Xu, Y. Zheng, Y. Shen, S. Liu, Y. Zhang, Bound oxygen-atom transfer endows peroxidase-mimic M-N-C with high substrate selectivity, Chem. Sci. 12 (2021) 8865.
[147] R.F. Zhang, X.Y. Yan, K.L. Fan, Nanozymes inspired by natural enzymes, Acc. Mater. Res. 2 (2021) 534.
[148] L. Huang, J. Chen, L. Gan, J. Wang, S. Dong, Single-atom nanozymes, Sci. Adv. 5 (2019), eaav5490.
[149] M.S. Kim, J. Lee, H.S. Kim, A. Cho, K.H. Shim, T.N. Le, S.S.A. An, J.W. Han, M.I. Kim, J. Lee, Heme cofactor-resembling Fe–N single site embedded graphene as nanozymes to selectively detect H_2O_2 with high sensitivity, Adv. Funct. Mater. 30 (2019), 1905410.
[150] Q. Zhou, H. Yang, X. Chen, Y. Xu, D. Han, S. Zhou, S. Liu, Y. Shen, Y. Zhang, Cascaded nanozyme system with high reaction selectivity by substrate screening and channeling in a microfluidic device, Angew. Chem., Int. Ed. Engl. 61 (2022), e202112453.
[151] W. Liu, H. Yang, Y. Ding, S. Ge, J. Yu, M. Yan, X. Song, Paper-based colorimetric immunosensor for visual detection of carcinoembryonic antigen based on the high peroxidase-like catalytic performance of $ZnFe_2O_4$-multi-walled carbon nanotubes, Analyst 139 (2014) 251.
[152] S. Ge, Y. Zhang, L. Zhang, L. Liang, H. Liu, M. Yan, J. Huang, J. Yu, Ultrasensitive electrochemical cancer cells sensor based on trimetallic dendritic Au@PtPd nanoparticles for signal amplification on lab-on-paper device, Sens. Actuators, B 220 (2015) 665.
[153] L. Liang, F. Lan, L. Li, M. Su, S. Ge, J. Yu, H. Liu, M. Yan, Fluorescence "turn-on" determination of H_2O_2 using multilayer porous SiO_2/NGQDs and PdAu mimetics enzymatic/oxidative cleavage of single-stranded DNA, Biosens. Bioelectron. 82 (2016) 204.
[154] Q. Kong, Y. Wang, L. Zhang, S. Ge, J. Yu, A novel microfluidic paper-based colorimetric sensor based on molecularly imprinted polymer membranes for highly selective and sensitive detection of bisphenol A, Sens. Actuators, B 243 (2017) 130.
[155] H. Mao, Z. Zuo, N. Yang, J.S. Huang, Y. Yan, A microfluidic colorimetric biosensor for chlorpyrifos determination based on peroxidase-like $CuFe_2O_4$/GQDs magnetic nanoparticles, J. Residuals Sci. Technol. 14 (2017) 255.
[156] N. Alizadeh, A. Salimi, R. Hallaj, Mimicking peroxidase activity of $Co_2(OH)_2CO_3$-CeO_2 nanocomposite for smartphone based detection of tumor marker using paper-based microfluidic immunodevice, Talanta 189 (2018) 100.
[157] S. Abarghoei, N. Fakhri, Y.S. Borghei, M. Hosseini, M.R. Ganjali, A colorimetric paper sensor for citrate as biomarker for early stage detection of prostate cancer based on peroxidase-like activity of cysteine-capped gold nanoclusters, Spectrochim. Acta, Part A 210 (2019) 251.
[158] N. Alizadeh, A. Salimi, R. Hallaj, Mimicking peroxidase-like activity of Co_3O_4-CeO_2 nanosheets integrated paper-based analytical devices for detection of glucose with smartphone, Sens. Actuators, B 288 (2019) 44.
[159] N. Fakhri, F. Salehnia, S. Mohammad Beigi, S. Aghabalazadeh, M. Hosseini, M.R. Ganjali, Enhanced peroxidase-like activity of platinum nanoparticles decorated on nickel- and nitrogen-doped graphene nanotubes: colorimetric detection of glucose, Microchim. Acta 186 (2019) 385.
[160] E. Ko, V.-K. Tran, S.E. Son, W. Hur, H. Choi, G.H. Seong, Characterization of Au@PtNP/GO nanozyme and its application to electrochemical microfluidic devices for quantification of hydrogen peroxide, Sens. Actuators, B 294 (2019) 166.
[161] C.A. Proenca, T.A. Baldo, T.A. Freitas, E.M. Materon, A. Wong, A.A. Duran, M.E. Melendez, G. Zambrano, R.C. Faria, Novel enzyme-free immunomagnetic microfluidic device based on $Co_{0.25}Zn_{0.75}Fe_2O_4$ for cancer biomarker detection, Anal. Chim. Acta 1071 (2019) 59.
[162] A. Bagheri pebdeni, M. Hosseini, Fast and selective whole cell detection of Staphylococcus aureus bacteria in food samples by paper based colorimetric nanobiosensor using peroxidase-like catalytic activity of DNA-Au/Pt bimetallic nanoclusters, Microchem. J. 159 (2020), 105475.
[163] N. Fakhri, S. Abarghoei, M. Dadmehr, M. Hosseini, H. Sabahi, M.R. Ganjali, Paper based colorimetric detection of miRNA-21 using Ag/Pt nanoclusters, Spectrochim. Acta, Part A 227 (2020), 117529.
[164] M.M. Liu, S.H. Li, D.D. Huang, Z.W. Xu, Y.W. Wu, Y. Lei, A.L. Liu, MoO_x quantum dots with peroxidase-like activity on microfluidic paper-based analytical device for rapid colorimetric detection of H_2O_2 released from PC12 cells, Sens. Actuators, B 305 (2020), 127512.
[165] F. Mesgari, S.M. Beigi, N. Fakhri, M. Hosseini, M. Aghazadeh, M.R. Ganjali, Paper-based chemiluminescence and colorimetric detection of cytochrome c by cobalt hydroxide decorated mesoporous carbon, Microchem. J. 157 (2020), 104991.
[166] Y. Hou, X. Guo, W. Liu, L. Zhang, C. Lv, Y. Jin, B. Li, X. Peng, Z. Zhang, Paper-based immunosensor with NH_2-MIL-53(Fe) as stable and multifunctional signal label for dual-mode detection of prostate specific antigen, J. Lumin. 230 (2021), 117708.
[167] Y. Huang, Y. Han, Y. Gao, J. Gao, H. Ji, Q. He, J. Tu, G. Xu, Y. Zhang, L. Han, Electrochemical sensor array with nanoporous gold nanolayer and ceria@gold corona-nanocomposites enhancer integrated into microfluidic for simultaneous ultrasensitive lead ion detection, Electrochim. Acta 373 (2021),

137921.
[168] W. Qi, L. Zheng, S. Wang, F. Huang, Y. Liu, H. Jiang, J. Lin, A microfluidic biosensor for rapid and automatic detection of *Salmonella* using metal-organic framework and Raspberry Pi, Biosens. Bioelectron. 178 (2021), 113020.
[169] N. Pazhoh, A. Badoei-dalfard, Z. Karami, Immobilization and biochemical characterization of choline oxidase onto bimetallic (Fe/Cu) MOF for sensitive determination of choline, J. Iran. Chem. Soc. (2022) 2795.
[170] J.S. Park, J.S. Choi, D.K. Han, Platinum nanozyme-hydrogel composite (PtNZHG)-impregnated cascade sensing system for one-step glucose detection in serum, urine, and saliva, Sens. Actuators, B 359 (2022), 131585.
[171] W. Qi, L. Zheng, Y. Hou, H. Duan, L. Wang, S. Wang, Y. Liu, Y. Li, M. Liao, J. Lin, A finger-actuated microfluidic biosensor for colorimetric detection of food-borne pathogens, Food Chem. 381 (2022), 131801.
[172] J. Zheng, M. Zhu, J. Kong, Z. Li, J. Jiang, Y. Xi, F. Li, Microfluidic paper-based analytical device by using Pt nanoparticles as highly active peroxidase mimic for simultaneous detection of glucose and uric acid with use of a smartphone, Talanta 237 (2022), 122954.
[173] B. Liu, J. Liu, Surface modification of nanozymes, Nano Res. 10 (2017) 1125.
[174] S. Li, Z. Zhou, Z. Tie, B. Wang, M. Ye, L. Du, R. Cui, W. Liu, C. Wan, Q. Liu, S. Zhao, Q. Wang, Y. Zhang, S. Zhang, H. Zhang, Y. Du, H. Wei, Data-informed discovery of hydrolytic nanozymes, Nat. Commun. 13 (2022) 827.
[175] H. Yin, D. Marshall, Microfluidics for single cell analysis, Curr. Opin. Biotechnol. 23 (2012) 110.
[176] C.L. Wang, W.T. Hu, L.D. Guan, X.P. Yang, Q.L. Liang, Single-cell metabolite analysis on a microfluidic chip, Chin. Chem. Lett. 33 (2022) 2883.
[177] M. Piergiovanni, S.B. Leite, R. Corvi, M. Whelan, Standardisation needs for organ on chip devices, Lab Chip 21 (2021) 2857.
[178] S. Jalili-Firoozinezhad, C.C. Miranda, J.M.S. Cabral, Modeling the human body on microfluidic chips, Trends Biotechnol. 39 (2021) 838.